




Please cite the Published Version

Al-Johani, Hanan, Haider, Julfikar , Satterthwaite, Julian  and Silikas, Nick  (2024) Lithium silicate-based glass ceramics in dentistry: a narrative review. *Prosthesis*, 6 (3). pp. 478-505.

DOI: <https://doi.org/10.3390/prosthesis6030034>

Publisher: MDPI AG

Version: Published Version

Downloaded from: <https://e-space.mmu.ac.uk/634580/>

Usage rights:  [Creative Commons: Attribution 4.0](https://creativecommons.org/licenses/by/4.0/)

Additional Information: This is an open access article which first appeared in *Prosthesis*, published by MDPI

Data Access Statement: The data presented in this study are available on request from the corresponding author.

Enquiries:

If you have questions about this document, contact openresearch@mmu.ac.uk. Please include the URL of the record in e-space. If you believe that your, or a third party's rights have been compromised through this document please see our Take Down policy (available from <https://www.mmu.ac.uk/library/using-the-library/policies-and-guidelines>)

Review

Lithium Silicate-Based Glass Ceramics in Dentistry: A Narrative Review

Hanan Al-Johani ^{1,2,*}, Julfikar Haider ^{1,3} , Julian Satterthwaite ¹  and Nick Silikas ¹ 

¹ Division of Dentistry, School of Medical Sciences, University of Manchester, Manchester M13 9PL, UK; j.haider@mmu.ac.uk (J.H.); julian.satterthwaite@manchester.ac.uk (J.S.); nikolaos.silikas@manchester.ac.uk (N.S.)

² Department of Restorative Dentistry, Division of Biomaterials, Faculty of Dentistry, King Abdulaziz University, Jeddah 21589, Saudi Arabia

³ Department of Engineering, Manchester Metropolitan University, Manchester M15 6BH, UK

* Correspondence: hamaljuhani1@kau.edu.sa

Abstract: Considering the rapid evolution of lithium silicate-based glass ceramics (LSCs) in dentistry, this review paper aims to present an updated overview of the recently introduced commercial novel LSCs. The clinical and in vitro English-language literature relating to the microstructure, manufacturing, strengthening, properties, surface treatments and clinical performance of LSC materials was obtained through an electronic search. Findings from relevant articles were extracted and summarised for this manuscript. There is considerable evidence supporting the mechanical and aesthetic competency of LSC variants, namely zirconia-reinforced lithium silicates and lithium–aluminium disilicates. Nonetheless, the literature assessing the biocompatibility and cytotoxicity of novel LSCs is scarce. An exploration of the chemical, mechanical and chemo-mechanical intaglio surface treatments—alternative to hydrofluoric acid etching—revealed promising adhesion performance for acid neutralisation and plasma treatment. The subtractive manufacturing methods of partially crystallised and fully crystallised LSC blocks and the additive manufacturing modalities pertaining to the fabrication of LSC dental restorations are addressed, wherein that challenges that could be encountered upon implementing novel additive manufacturing approaches using LSC print materials are highlighted. Furthermore, the short-term clinical performance of zirconia-reinforced lithium silicates and lithium–aluminium disilicates is demonstrated to be comparable to that of lithium disilicate ceramics and reveals promising potential for their long-term clinical performance.

Keywords: lithium silicate-based glass ceramics; CAD/CAM; crystallisation; surface treatments



Citation: Al-Johani, H.; Haider, J.; Satterthwaite, J.; Silikas, N. Lithium Silicate-Based Glass Ceramics in Dentistry: A Narrative Review. *Prosthesis* **2024**, *6*, 478–505. <https://doi.org/10.3390/prosthesis6030034>

Academic Editors: Roberto Sorrentino, Fernando Zarone and Gennaro Ruggiero

Received: 6 April 2024
Revised: 21 April 2024
Accepted: 25 April 2024
Published: 2 May 2024



Copyright: © 2024 by the authors. Licensee MDPI, Basel, Switzerland. This article is an open access article distributed under the terms and conditions of the Creative Commons Attribution (CC BY) license (<https://creativecommons.org/licenses/by/4.0/>).

1. Introduction

Lithium silicate-based glass ceramics (LSCs) were first identified by Stookey [1] in 1959 from precipitations of lithium disilicate crystals in glass and nucleating clusters of Ag, forming a binary lithium disilicate glass ceramic system; this was subsequently reformulated by Beall [2] into a multi-component lithium disilicate and lithium metasilicate system. Later Ivoclar Vivadent (Schaan, Liechtenstein) introduced two pressable LSCs, IP Empress 2 (1998) and IPS e.max Press (2005), along with a machinable LSC block, IPS e.max CAD (2006) [3]. As a measure of the clinical success of its lithium disilicate formulation, Ivoclar Vivadent delivered 75 million IPS e.max Press and IPS e.max CAD restorations from 2005 to 2013 [4]. This success encouraged competing manufacturers to develop a plethora of commercial LSCs with patented chemical compositions and strengthening mechanisms in pressable and machinable formats [5]. In 2013, machinable zirconia-reinforced lithium silicates were developed by VITA Zahnfabrik (Bad Säckingen, Germany) and Dentsply Sirona (Salzburg, Austria) in the form of VITA Suprinity and Celtra Duo, respectively [6], and pressable versions were later introduced (Celtra Press, Dentsply Sirona, Salzburg, Austria, 2017 and VITA AMBRIA, VITA Zahnfabrik, Bad Säckingen,

Germany, 2021). Moreover, lithium–aluminium disilicates were offered as fully crystallised CAD/CAM blocks, namely n/ce, by Straumann (Basel Switzerland) in 2017, and CEREC Tessera was developed by Dentsply Sirona (Salzburg, Austria) in 2021 [4,7]. Recent in vitro investigations by Ivoclar Vivadent explored the effects of incorporating lithium tantalate and lithium niobate precipitations in LSC formulations and reported positive findings for future material development [8–10]. Considering the similar coefficients of thermal expansion of LSCs and zirconia, novel LSC spray deposition has been advocated as a promising surface pre-treatment for zirconia restorations in an attempt to obtain favourable characteristics from both materials as well as to enhance the bond strength between zirconia and underlying resin cement [11–13].

Tables 1 and 2 highlight the composition, flexural strength and clinical indications of pressable and CAD/CAM LSCs that are currently commercially available.

Table 1. Composition, flexural strength and clinical indications of pressable lithium silicate-based ingots as published by representative manufacturers.

Ceramic Type	Product Name, Manufacturer (Launch Date)	Chemical Composition (wt%)	Flexural Strength (MPa)	Clinical Indications
Lithium-disilicate (Li ₂ Si ₂ O ₅)	IPS e.max [®] Press, Ivoclar Vivadent, Schaan, Liechtenstein (2005)	SiO ₂ (57.0–80.0), Li ₂ O (11.0–19.0), K ₂ O (<13.0), P ₂ O ₅ (<11.0) ZrO ₂ (<8.0), ZnO (<8.0), colouring oxides (<12.0)	470	Inlays, onlays, veneers, crowns, 3-unit FPDs up to 2nd premolar, implant-supported crowns
	Initial TM LiSi Press, GC Corp., Tokyo, Japan (2016)	SiO ₂ (71.0), Li ₂ O (13.0), Al ₂ O ₃ (5.4), Na ₂ O (1.4), K ₂ O (2.0), P ₂ O ₅ (2.6), ZrO ₂ (1.7), B ₂ O ₃ (0.007), CeO ₂ (1.2), V ₂ O ₅ (0.15), Tb ₂ O ₃ (0.35), Er ₂ O ₄ (0.4), HfO ₂ (0.03)	508	Inlays, onlays, veneers, anterior and posterior crowns, implant crowns, 3-unit FPDs on teeth or implants up to 2nd premolar
	Amber [®] Press, HASS Corp., Gangwon State, Korea (2020)	SiO ₂ (<78), Li ₂ O (<12), colouring oxides (<12)	460	Inlays, onlays, veneers, anterior and posterior crowns, 3-unit FPDs on teeth up to 2nd premolar
	Livento Press, Cendres + Métaux, Biel/Bienne, Switzerland (2019)	SiO ₂ (65–80), Al ₂ O ₃ (<11), Li ₂ O (11–19), K ₂ O (<7), Na ₂ O (<5), CaO (<10), P ₂ O ₅ (1.5–7), ZnO (<7), others (<15)	300	Inlays and onlays, veneers, partial crowns, anterior and posterior crowns, hybrid abutment crowns, 3-unit anterior and posterior bridges up to 2nd premolar
Zirconia reinforced lithium silicates (Li ₂ SiO ₃ /Li ₂ Si ₂ O ₅)	Celtra [®] Press, Dentsply Sirona, Salzburg, Austria (2017)	SiO ₂ (58), Li ₂ O (18.5), ZrO ₂ (10.1), P ₂ O ₅ (5), Al ₂ O ₃ (1.9), CeO ₂ (2), Tb ₄ O ₇ (1)	>500	Inlays, onlays, veneers, anterior and posterior crowns, 3 unit anterior bridges
	VITA AMBRIA [®] , VITA Zahnfabrik, Bad Säckingen, Germany (2021)	SiO ₂ (58–66), Li ₂ O (12–16), Al ₂ O ₃ (1–4), K ₂ O (1–4), P ₂ O ₅ (2–6), ZrO ₂ (8–12), B ₂ O ₃ (1–4), CeO ₂ (<4), V ₂ O ₅ (<1) Tb ₂ O ₃ (1–4), Er ₂ O ₄ (<1), Pr ₆ O ₁₁ (<1)	400	Inlays, onlays, veneers, anterior and posterior crowns, implant crowns, 3-unit FPDs on teeth or implants up to 2nd premolar

Table 2. Composition, flexural strength and clinical indications of CAD/CAM lithium silicate-based blocks as published by representative manufacturers.

Ceramic Type	Product Name, Manufacturer (Launch Date)	Chemical Composition (wt.%)	Flexural Strength (MPa)	Processing	Clinical Indications
Lithium-disilicate (Li ₂ Si ₂ O ₅)	IPS e.max® CAD, Ivoclar Vivadent, Schaan, Liechtenstein (2006)	SiO ₂ (57.0–80.0), Li ₂ O (11.0–19.0), K ₂ O (<13), P ₂ O ₅ (<11), ZrO ₂ (<8.0), ZnO (<8.0), Al ₂ O ₃ (<5.0), MgO (<5.0), pigments (<0.8)	360 ± 40	Two-step	Inlays, onlays, veneers, anterior and posterior crowns, 3-unit FPDs up to 2nd premolar, implant supported crowns
	Rosetta SM, HASS Corp., Gangwon State, Korea (2013)	SiO ₂ (<78), Li ₂ O (<120, colouring oxides (<12)	400	Two-step	Inlays, onlays, veneers, anterior and posterior crowns, 3-unit anterior FPDs
	Amber® Mill, HASS Corp., Gangwon State, Korea (2018)	SiO ₂ (<78), Li ₂ O (<12), colouring oxides (<12)	450	Two-step	Inlays, onlays, veneers, anterior and posterior crowns, 3-unit FPDs (up to 2nd premolar)
	Initial™ LiSi Blocks, GC Corp., Tokyo, Japan (2021)	SiO ₂ (81), P ₂ O ₅ (8.1), K ₂ O (5.9), Al ₂ O ₃ (3.8), TiO ₂ (0.5), CeO ₂ (0.6)	408	One-step	Inlays, onlays, veneers, anterior and posterior crowns, implant-supported crowns
Lithium-metasilicate (Li ₂ SiO ₃)	Obsidian®, Glidewell Laboratories, CA, USA (2013)	SiO ₂ (50–58), Li ₂ O (10–20), GeO ₂ (1–10), K ₂ O (2–6), P ₂ O ₅ (2–4), Al ₂ O ₃ (2–4), ZrO ₂ (2–4), others (<10)	385	Two-step	Inlays, onlays, veneers, anterior and posterior crowns
Zirconia reinforced lithium silicates (Li ₂ SiO ₃ /Li ₂ Si ₂ O ₅)	Celtra® Duo, Dentsply Sirona, Salzburg, Austria (2013)	SiO ₂ (58), Li ₂ O (18.5), ZrO ₂ (10.1), P ₂ O ₅ (5), Al ₂ O ₃ (1.9), CeO ₂ (2), Tb ₄ O ₇ (1)	370	One-step	Inlays, onlays, veneers, partial crowns, anterior and posterior crowns, implant-supported crowns
	VITA Suprinity®, VITA Zahnfabrik, Bad Säckingen, Germany (2013)	SiO ₂ (56–64), Li ₂ O (15–21), ZrO ₂ (8–12), P ₂ O ₅ (3–8), Al ₂ O ₃ (1–4), K ₂ O (1–4), CeO ₂ (<4), La ₂ O ₃ (0.1), pigments (<6)	420	Two-step	Inlays, onlays, veneers, partial crowns, anterior and posterior crowns, implant-supported crowns
Lithium aluminium disilicate (LiAlSi ₂ O ₆ /Li ₂ Si ₂ O ₅)	n!ce®, Straumann, Basel, Switzerland (2017)	SiO ₂ (64–70), Li ₂ O (10.5–12.5), Al ₂ O ₃ (10.5–11.5), Na ₂ O (1–3), K ₂ O (0–3), P ₂ O ₅ (3–8), ZrO ₂ (<0.5), CaO (1–2), colouring oxides (<9)	350 ± 50	One-step	Inlays, onlays, veneers, anterior and posterior crowns, implant-supported crowns
	CEREC Tessera™, Dentsply Sirona, Salzburg, Austria (2021)	Li ₂ Si ₂ O ₅ (90), Li ₃ PO ₄ (5), Li _{0.5} Al _{0.5} Si _{2.5} O ₆ (5)	700	Two-step	Inlays, onlays, veneers, anterior and posterior crowns

Previous existing review papers in the literature have investigated the chemical, aesthetic and mechanical aspects that govern the performance of recent LSC materials [5–7,14,15], while others have evaluated the outcomes of internal surface treatments on LSC cementation and adhesion [14,16]. The main aim of this narrative review is to shed light on the manufacturing and strengthening methodologies of the notably recent LSC materials pertaining to dental applications and to consolidate a comprehensive understanding of the updated fabrication techniques and surface treatment modalities available in the literature to enhance the knowledge of dental practitioners regarding the contemporary developments in this rapidly evolving field. The review methodology herein comprises applying a search strategy (Table 3), defining inclusion and exclusion criteria, screening relevant abstracts, retrieving the full text of studies from selected abstracts and extracting the main outcomes/findings. Inclusion selection criteria were articles written in English and related to LSC materials, including in vitro studies (comparative or experimental), technique reports, review articles, case reports and clinical studies. Exclusion criteria included any articles that failed to align with the items described in the inclusion criteria. Electronic searches included research in the literature published until February 2024.

Table 3. Search strategy for narrative review.

Database	Search Terms
Pubmed/ Medline	“Lithium silicate-based glass-ceramics” OR “Lithium disilicate” OR “Zirconia-reinforced lithium silicate” OR “Lithium aluminum disilicate” OR “Advanced lithium disilicate” OR “Glass-ceramics” OR “Dental ceramics” OR “dental materials” [Mesh] OR “dentistry” [Mesh] OR “CAD/CAM” [Mesh] OR “machinable lithium silicate” OR “pressable lithium silicate” OR “heat pressed lithium silicate”
Scopus	“Lithium AND silicate-based AND dental AND ceramics” OR “Zirconia-reinforced AND lithium AND silicate” OR “Advanced AND lithium AND disilicate” OR “Reinforced AND lithium AND silicate” OR “CAD/CAM AND lithium AND silicate” OR “Heat AND pressed AND lithium AND silicate”
Google Scholar	“Lithium silicate-based glass-ceramics” OR “Lithium disilicate” OR “Zirconia-reinforced lithium silicate” OR “Lithium aluminum disilicate” OR “Advanced lithium disilicate” OR “Glass-ceramics” OR “CAD/CAM lithium silicates” OR “machinable lithium silicate” OR “pressable lithium silicate” OR “heat pressed lithium silicate”

2. Microstructure

The microstructure of LSCs comprises lithium disilicate crystals (≥ 50 vol%) formed via volume crystallisation with phosphorus pentoxide (P_2O_5) as their primary nucleant and (in some derivatives) zirconia (ZrO_2) as a secondary nucleating agent [2,17]. Lithium (Li) was initially extracted from silicate mineral petalite ($LiAlSi_4O_{10}$) and later from spodumene ($LiAlSi_2O_6$). LSCs consist of three main silicate forms (Figure 1):

1. Lithium disilicate ($Li_2Si_2O_5$): a layered silicate (i.e., phyllosilicate) in which silicon shares three oxygen atoms with its neighbouring atoms; this phase exists between 800 and 850 °C;
2. Lithium metasilicate (Li_2SiO_3): a single-chain silicate (i.e., inosilicate) where silicon shares only two oxygen atoms; this phase is metastable and exists exclusively between 600 and 800 °C;
3. Cristobalite (SiO_2): a stable silica framework, i.e., tectosilicate, in which silicon shares all four oxygen atoms; this secondary phase crystallises following that of $Li_2Si_2O_5$.

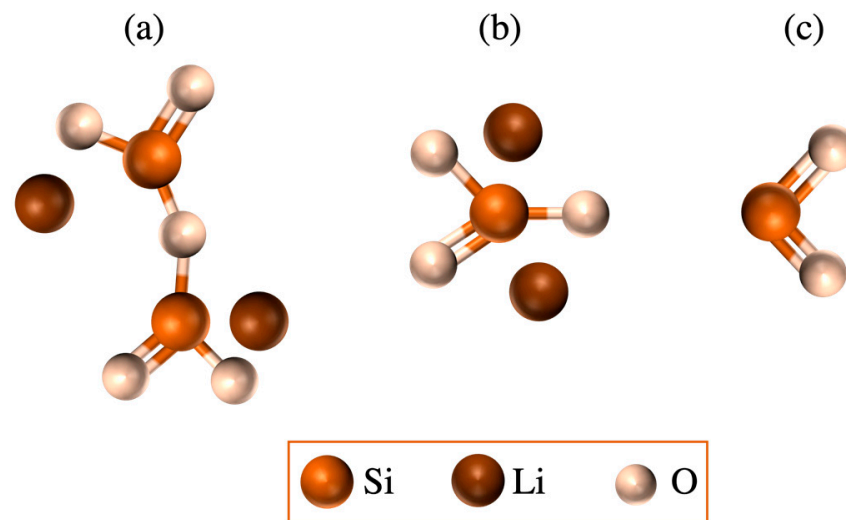
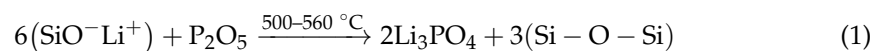


Figure 1. Molecular representation of (a) lithium disilicate, (b) lithium metasilicate and (c) cristobalite.

The microstructure of LSCs is governed by heterogeneous nucleation via a micro immiscibility approach where foreign substrates are integrated within a glass matrix and create a microphase that acts as a heterogenous nucleating agent. Microphases gain kinetic energy upon heating, promoting crystal growth, phase separation and the development of additional crystal phases. Phosphorus pentoxide (P_2O_5) is considered the main LSC nucleant, and supplemental oxides (e.g., Al_2O_3 , K_2O , ZrO_2 , ZnO , MgO and CeO_2) are added as secondary nucleating agents, fluxes or fining agents to accelerate crystallisation kinetics, control melting temperatures and viscosity and improve corrosion resistance [18–20]. Heating LSCs with P_2O_5 (>2 mol%) to 500–560 °C results in lithium orthophosphate (Li_3PO_4) and cristobalite (SiO_2) [20]:



Li_3PO_4 serves as a heterogeneous nucleus initiating the layered deposition (i.e., epitaxial growth) of lithium metasilicate crystals (Li_2SiO_3) starting from 530 to 590 °C until they decompose at 780–820 °C. Cristobalite crystals also decompose below 820 °C; concurrently, lithium disilicate ($Li_2Si_2O_5$) crystals start growing in a rapid manner at 820 °C [20]:



The elongated morphology of $Li_2Si_2O_5$ crystals (i.e., high aspect ratio) toughens LSCs by virtue of crack deflection and crack bridging mechanisms [19]. Furthermore, the resultant LSC crystalline structure is a remarkably interlocked crystal network, and its epitaxial crystal growth relies on the minimal distance (<15%) between the nuclei lattices and growing crystals; fortunately, this is easily attained by the similar orthorhombic structures of Li_3PO_4 and Li_2SiO_3 [20]. Furthermore, in general, LSCs are considered to be multi-component and non-stoichiometric (i.e., with non-ratio atomic relationships within its elemental composition) and thereby can be further divided based on the dominance of the microstructural phase/phases [4,5] into four sub-classes:

Lithium disilicate ceramic (LDS): predominantly lithium disilicate ($Li_2Si_2O_5$);

Lithium metasilicate ceramic (LM): predominantly lithium metasilicate (Li_2SiO_3);

Zirconia-reinforced lithium silicate (ZLS): biphasic lithium metasilicate/lithium disilicate ($Li_2SiO_3/Li_2Si_2O_5$);

Lithium aluminium disilicate (ALD): biphasic spodumene/lithium disilicate ($LiAlSi_2O_6/Li_2Si_2O_5$).

The majority of the CAD/CAM LSCs in the market (IPS e.max CAD, Rosetta SM, Amber Mill, Obsidian and VITA Suprinity) are available as partially crystallised blocks from Li_2SiO_3 to facilitate their soft-milling, and then undergo mandatory crystallisation and glaze firing protocols at higher temperatures ($>800^\circ\text{C}$) for Li_2SiO_3 phase transformation into the desired $\text{Li}_2\text{Si}_2\text{O}_5$ crystalline structure. In the pre-sintered state, IPS e.max CAD blocks demonstrate low mechanical properties; however, upon sintering and crystallisation, the strength of the ceramic blocks improves tremendously [3]. More recently, attempts in limiting the CAD/CAM fabrication time have led to the development of fully crystallised LSC blocks either with post-milling glaze firing regimens (Celtra Duo and CEREC Tessera) or without glaze firing prerequisites (Initial LiSi Block and n!ce) [4,7].

2.1. Zirconia-Reinforced Lithium Silicate Ceramics (ZLSs)

The unique microstructure of these ceramics is due to the tetragonal zirconia fillers (ZrO_2) added in concentrations of ~ 10 wt% in the glassy matrix, serving as a secondary nucleant to diphosphorus pentoxide (P_2O_5) (Figure 2) [21]. Currently, commercial ZLSs are offered as pressable ingots, including Celtra Press (Dentsply Sirona, Salzburg, Austria) and VITA AMBRIA (VITA Zahnfabrik, Bad Säckingen, Germany), as well as machinable blocks in a fully crystallised form, e.g., Celtra Duo (Dentsply Sirona, Salzburg, Austria), and in a partially crystallised form, e.g., VITA Suprinity (VITA Zahnfabrik, Bad Säckingen, Germany) [7]. The partially crystallised ZLS machinable blocks (VITA Suprinity, VITA Zahnfabrik, Bad Säckingen, Germany) are composed of pre-sintered Li_2SiO_3 nanocrystals embedded within moderately polymerised zirconosilicate glass. Upon heating the block to 810 – 820°C , the Li_2SiO_3 crystals react with the glass to generate $\text{Li}_2\text{Si}_2\text{O}_5$ (major) and Li_3PO_4 (minor) precipitates, resulting in a ~ 60 vol% crystalline phase with an average crystal size of 0.5 – $1\ \mu\text{m}$ being incorporated in a zirconosilicate glass matrix [4,6,21,22]. This intricate microstructure provides the ZLSs with superior flexural strength, and improved aesthetics and machinability because of the higher percentage of the glassy matrix [23]. In vitro chewing simulation and artificial ageing studies conducted by the manufacturers of Celtra Duo (Dentsply Sirona, Salzburg, Austria) [24] claim that these ceramics behave in an uncharacteristic manner in which they gain strength upon hydrothermal ageing. Other published studies have explained this on the basis of zirconia phase transformation from tetragonal crystals into monoclinic ones, thereby resulting in crack retardation and, in turn, higher fracture loads [25–27]. X-ray diffraction (XRD) investigations have been employed to identify and quantify the crystalline structures within ZLS, while some researchers have not detected crystalline zirconia structures [21,28], but others have identified tetragonal ZrO_2 crystals and aluminium silicate (VITA Suprinity, VITA Zahnfabrik, Bad Säckingen, Germany) after sintering at 840°C [29], and extended firing at $>875^\circ\text{C}$ [18].

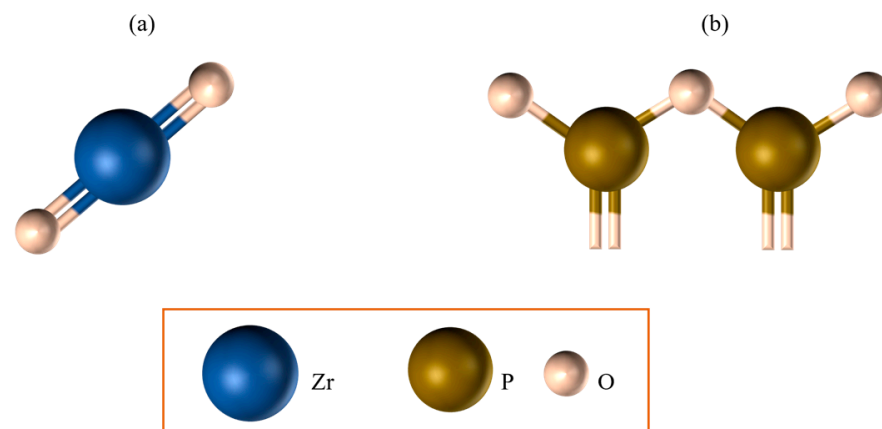


Figure 2. Molecular representation of nucleating agents: (a) zirconia and (b) diphosphorus pentoxide.

2.2. Lithium–Aluminium Disilicates (ALDs)

ALDs were initially introduced by Straumann (Basel Switzerland) as one of the n!ce products, distinguished by the high density of β -spodumene ($\text{LiAlSi}_2\text{O}_6$) (~41 vol%) in addition to $\text{Li}_2\text{Si}_2\text{O}_5$ (28.5 vol%) and Li_3PO_4 (~10 wt%) [5,7] (Figure 3). The most recent ALD materials (CEREC Tessera) are advertised as “advanced lithium disilicates”, ostensibly due to the manufacturer (Dentsply Sirona, Salzburg, Austria) marketing of added Al_2O_3 content (~5 wt%) in the form of γ -spodumene, i.e., virgilite crystals ($\text{Li}_{0.5}\text{Al}_{0.5}\text{Si}_{2.5}\text{O}_6$), as well as $\text{Li}_2\text{Si}_2\text{O}_5$ (~90 wt%) and Li_3PO_4 (~5 wt%). Toughening of CEREC Tessera occurs as a result of the thermal mismatch between $\text{Li}_{0.5}\text{Al}_{0.5}\text{Si}_{2.5}\text{O}_6$ and $\text{Li}_2\text{Si}_2\text{O}_5$ crystals, which both form between 800 and 850 °C, causing residual stresses and crack tip shielding upon cooling of the ALD [7,30]. However, XRD investigations [5,31] obtained from Rietveld refinement have refuted this claim, stating that instead of virgilite, the crystalline content is composed of quartz (~3 vol%). Although ALDs are currently supplied as fully crystallised CAD/CAM blocks that can be cemented post-milling without further heating or glaze treatment requirements, evidence in the literature suggests that additional sintering is beneficial in minimising milling-induced surface flaws [7].

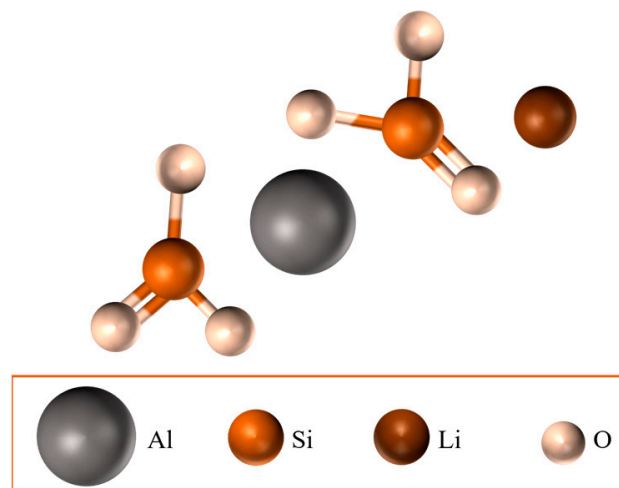


Figure 3. Molecular representation of spodumene.

3. Manufacturing Techniques

The manufacturing of LSC materials is achieved through consolidating and heating ceramic powders by virtue of complex temperature-controlled crystallisation methods.

3.1. Melting Casting Crystallisation Method

Raw glass-forming components and nucleating agents are uniformly mixed and simultaneously melted at high temperatures ranging between 1300 and 1500 °C. The molten glass is quenched via casting it into the desired geometry and slowly cooling it at room temperature, i.e., it is annealed to form a precursor glass. Subsequently, a two-stage controlled heat treatment takes place, initially at temperatures slightly above the glass transition temperature (T_g), to stimulate nucleation; then, the temperature is raised in a second heating stage to facilitate the stable growth of crystals of minimal inherent stresses within the precursor glass. The final microstructure depends on the type and concentration of nucleating agents as well as the dimension and shape of the crystals (Figure 4). Complex geometries can be manufactured using this method, yielding uniformly dense compositions with accurate dimensions. However, as melting temperatures can be reduced via the addition low-melting-temperature oxides, the overall high temperatures and prolonged treatment time are considered limitations of this approach [32–35].

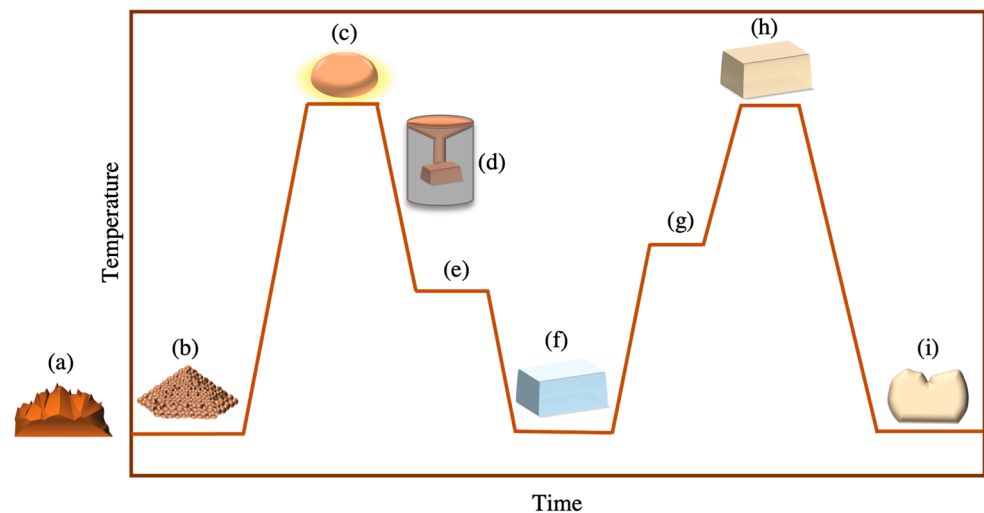


Figure 4. Melting casting crystallisation manufacturing method; raw minerals (a) are milled into fine powders (b), mixed, then heated into a molten state (c), quenched and cast within a mould (d), slowly annealed (e) to form a precursor glass (f), re-heated to illicit nucleation, (g) re-heated a second time to active crystallisation kinetics (h) and finally cooled slowly to obtain a glass ceramic with optimum properties (i).

3.2. Powder Sintering Method

This method attempts to speed up manufacturing through the coincident sintering and crystallisation of glass particles; the raw glass materials are melted at high temperatures, quenched in water, finely ground into a powder, sieved in a blank and pressed at specific temperatures. The final crystalline structure is achieved via bulk nucleation along the glass grain border without the need for additional nucleating agents. This approach is less complex and time-consuming than the melting casting method and allows for the production of high-temperature fused glasses that cannot easily form a molten glass phase. However, a significant drawback is the resultant inherent porosity, which limits the fabrication of geometrically intricate configurations [32–36].

3.3. Sol–Gel Method

Hydrolysis is employed to create a gel from glass element precursors that is then dried into glass powder, moulded and sintered at reduced temperatures (600–800 °C). The main advantages of this method are the nano-scaled dimensions of glass particles that enhance the homogeneity of the final product, and that lower temperatures prevent the possible volatilisation of glass particles, thus reducing contamination. Nonetheless, this approach is time-consuming and expensive, and the sintering shrinkage of the gel poses a potential risk [32,35,37].

4. Strengthening Mechanisms

Owing to their brittle nature, LSCs cannot plastically deform to dissipate pre-existent internal dislocation energy, which could thus potentially result in catastrophic cleavage. Manufacturing processes inevitably generate critical flaws (inherent bulk flaws or outer surface defects) that act as strength-limiting zones of high-stress concentrations. The stochastic fracture behaviour of LSCs is thus due to the multi-fold randomly distributed critical flaws from which cracks of differing dimensions and orientations initiate and, subsequently, propagate. Ultimately, crack progression is governed by the size effect and weakest link theory postulating that cracks originate from the largest flaws oriented in a manner susceptible to the alignment of weakening tensile stresses [38–41]. Thus, the strengthening or toughening of LSCs is imperative to providing longevity and can be performed via a variety of intrinsic or extrinsic mechanisms [41–44]; the former focuses on

inherent processes located within the crack tip vicinity (Figure 5), whereas the latter are acquired processes that impede the driving force behind the extension of a crack.

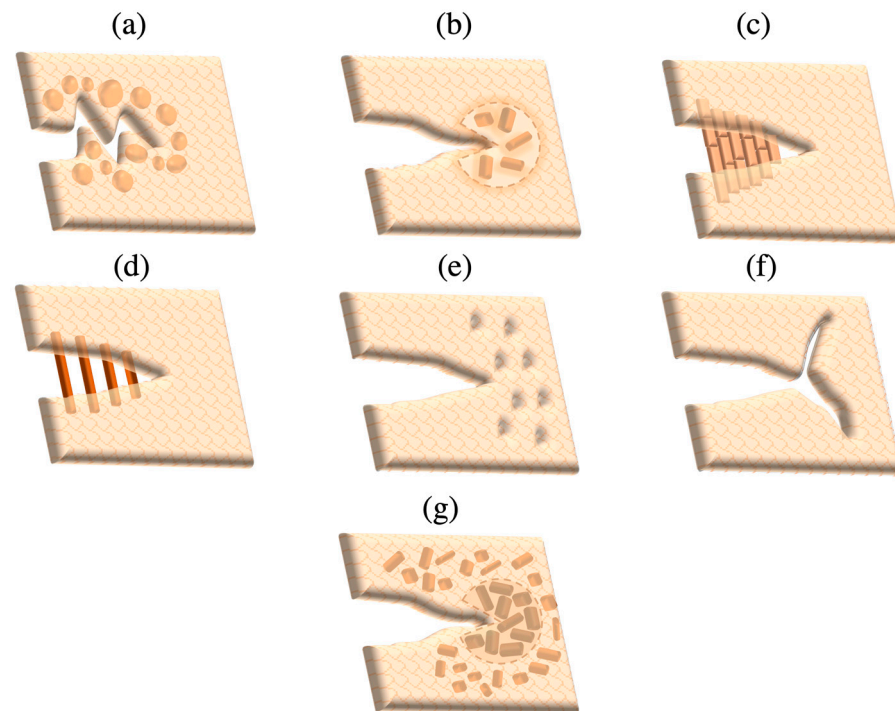


Figure 5. LSC intrinsic strengthening mechanisms: (a) crack tip deflection, (b) crack tip shielding, (c) grain bridging, (d) fibre bridging, (e) microcracks, (f) crack branching and (g) transformation toughening.

Intrinsic strengthening mechanisms

- Crack tip deflection: Added particles in the glass matrix act as obstacles deflecting the crack into an altered plane, increasing the surface area per distance of the crack and consequently causing crack advancement to be decelerated as extra energy is needed for its propagation.
- Crack tip shielding: This is triggered by high stresses within the crack tip vicinity, where residual stresses arise from mismatches in the coefficients of thermal expansion (CTE) between crystalline particles and the glass matrix; the greater CTE of crystals than that of the surrounding glass matrix stimulates compressive stresses at the crack tip that minimise its opening.
- Crack bridging: In ceramic networks of high crystalline density, cracks spread in an inter-granular manner, thereby causing friction to be generated between the grains along crack surfaces, triggering grain pull-out, frictional interlocking and bridging, and thus impeding further crack extension. Bridging can also be accomplished via the reinforcement of added fibres or whiskers within the ceramic matrix.
- Microcrack formation and crack branching: Concentrated stress around the crack tip generates microcracks within adjacent inherent flaws and grain boundaries oriented perpendicularly to the stress plane. Microcracks dissolve the crack expansion energy within the tip region, thereby hindering further crack advancement. Branching at the crack tip also acts to delay crack motion by increasing the crack surface area.
- Transformation toughening: Stresses surrounding the crack tip region prompt crystalline phase transformations that are accompanied by volumetric expansion exerting favourable compressive residual stresses coalescing the crack tip.

Extrinsic strengthening mechanisms

- **Thermal tempering:** This involves the controlled heating of a ceramic to a temperature that is slightly above the glass transition point (T_g) and beneath the softening point (T_s), creating a rigid exterior surface that envelopes a molten centre [45]. Upon cooling, the molten core contracts and a temperature gradient is generated between the surface and bulk, yielding residual compressive stresses within the former and inner residual tensile stresses within the latter (Figure 6). Therefore, to fracture tempered ceramic restorations, externally applied tensile loads must counter the residual compressive stresses of the ceramic surface.

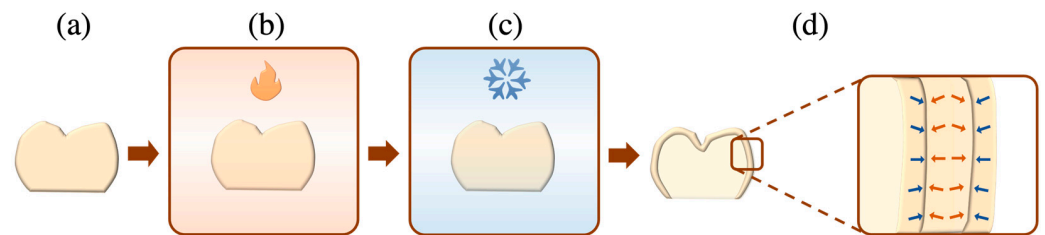


Figure 6. Thermal tempering of a ceramic restoration (a), placed in a furnace, initially heated to a temperature between its T_s and T_g (b), and then cooled rapidly via assisted forced air cooling (c). The final tempered ceramic has two-fold residual stresses: outer compressive stresses (blue arrows) and inner tensile stresses (orange arrows) (d).

- **Chemical tempering:** This is also known as ion exchange or ion stuffing, where the exchange of different sized ions at the outer ceramic surfaces yields residual compressive stresses as the larger ions swap those of smaller sizes. This is achieved via the immersion of the LSC in a molten potassium nitrate (KNO_3) salt bath; smaller-sized ions on the LSC surface (e.g., Na^+ and Li^+) are substituted by larger ions in the salt bath (e.g., K^+). The resultant chemically tempered ceramics are electroneutral by virtue of the equivalent counter ion flux diffusion (Figure 7) [43,46,47].

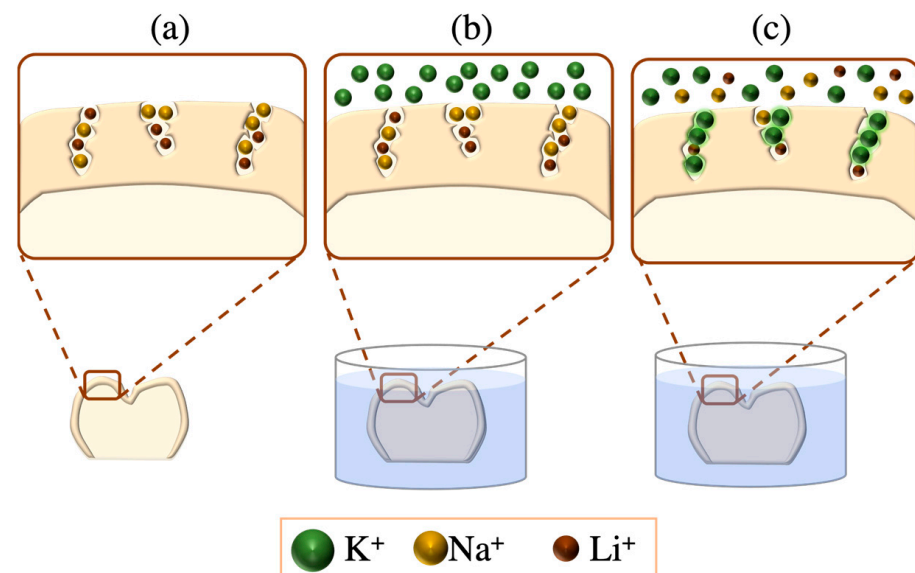


Figure 7. Chemical tempering of a lithium-based ceramic restoration composed of small-sized Na^+ and Li^+ ions within its silicate network (a). The ceramic is heated ($T < T_g$) within a salt bath saturated with large-sized K^+ ions (b). An Ion exchange proceeds as Na^+ and Li^+ ions are replaced with K^+ ions; the latter generates favourable compressive stresses throughout the silicate framework that retard the propagation of pre-existing crack (c).

5. Fabrication Methods

Currently, various LSC dental restorations can be fabricated via one of the following methods.

5.1. Heat Pressing

Also known as injection moulding, this method utilises the lost wax technique in which a wax model of an LSC restoration is embedded in gypsum materials to create a mould. Subsequently, LSC ingots are heated to a temperature at which they melt into a highly viscous liquid, allowing them to be pressed/injected into the lost wax mould cavity. This fabrication method allows the production of full-contour restorations as well as frameworks designed to be veneered with feldspathic porcelain. The benefit of this technique is its resemblance to and familiarity with the lost wax method used to produce metal castings, therefore minimising potential laboratory mishaps [48,49].

5.2. CAD-CAM Technology

This method is conducted throughout three main processes:

1. Data acquisition: The prepared abutment teeth and their surrounding tissues are recorded indirectly via conventional dental impressions or directly through virtual impressions [50,51];
2. Data processing and computer-aided design: Software programs transfer the acquired data to a processing centre, and the desired restoration is created [50–52] with the aid of software tools such as smile design, tooth form libraries, colour shade matching and jaw tracking programs [53];
3. Computer-aided manufacturing: Upon finalising the LSC restoration design, it can be manufactured via subtractive (SM), additive (AM) or hybrid SM and AM mechanisms.

5.2.1. Subtractive Manufacturing

Herein, the LSC block (partially or fully sintered) is fixed onto a workpiece and a milling drill (spindle) subtracts from the material to create the desired restoration. Subtractive manufacturing is executed by a computer numeric-controlled (CNC) milling machine with a series of successive commands regarding the milling tool type, path and speed, as regulated by the thickness and morphology of the desired restoration. Within most CNC milling systems in dentistry, milling burs operate along 3 or 4 defined axes, with 5-axis milling machines being less common (Figure 8):

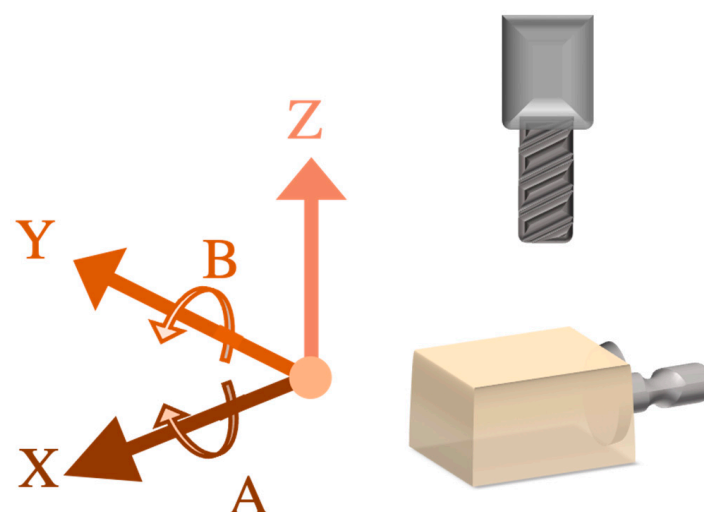


Figure 8. Depiction of the axis orientation in subtractive manufacturing; the milling bur moves along the Z-axis, whereas the LSC block moves along the X-, A-, Y- and B-axes.

Three-axis devices function within XYZ spatial paths; the workpiece moves horizontally in the X-axis (left/right) and Y-axis path (forward/backward), and the spindle moves vertically along the Z-axis (up/down). These systems require minimal control and can fabricate restorations in a short milling time with low costs; hence, they are the most popular in dental clinics. However, internal fit and marginal adaptation are frequent concerns. Four-axis milling devices have an additional rotational axis: an A-axis, which pertains to the X-axis, allowing the workpiece to move in a pendulum-like fashion, thereby exposing greater surfaces to be milled by the spindle and allowing access to the undercut areas of the restorations; nonetheless, these devices are less widespread in the dental field due to their higher costs. In terms of 5-axis milling devices, there is an added rotational axis: a B-axis, which relates to the Y-axis, in addition to the XYZA axes. The automated maturity of these systems facilitates the efficient milling of surfaces adjacent to the insertion axis with an accuracy of up to 0.01 mm; nonetheless, their large footprint and financial restraints limit their placement to external laboratories only. The indication of 3- and 4-axis systems are limited to single-unit or short-multi-unit prostheses, whereas 5-axis systems can fabricate long-span multi-unit and geometrically complex restorations [54]. Subtractive manufacturing has increasingly gained popularity within the last decade; however, milling-induced strength-limiting surface flaws and material wastage are significant drawbacks [53–57].

5.2.2. Additive Manufacturing

LSC restorations are constructed as a function of a structured passive layering technique guided by the information from the three-dimensional design data, yielding less material waste, and thus endorsing industrial sustainability. The unique software algorithms of additive manufacturing can generate multi-shade prostheses of geometric complexity. In contrast to subtractive approaches, additive manufacturing allows the fabrication of larger-sized structures with extensive surface irregularities; therefore, it is preferred for the construction of extra-oral hard- and soft-tissue facial prostheses. This can be accomplished using seven main technologies [58–60]:

1. Material jetting (MJ): This is also recognised as direct inkjet printing, in which a layer of tiny droplets of the print material (i.e., ink) are selectively deposited onto a build platform, where the latter is heated or exposed to ultraviolet (UV) radiation to facilitate immediate photopolymerisation of the jetted layer ink before the subsequent ink layer is added. Ceramic particles can be suspended into water, organic solvents or wax solutions to create the ceramic ink needed to fabricate dental restorations via the material jetting method.
2. Vat polymerisation (VP): This entails the selective photocuring of radiation-sensitive liquid polymers contained within a tank (i.e., vat). This is the most frequently used additive method for fabricating dental ceramics, wherein ceramic suspensions are developed through the incorporation of resin polymers in high concentrations within ceramics powders. VP can be further subdivided into three main technologies; stereolithography (in which a concentrated UV-laser beam is directed onto a photosensitive liquid resin generating layers of the desired object through the crosslinking of the polymers), digital light processing (a digital UV screen simultaneously deposits and photocures an entire layer of photopolymerisable liquid) and continuous liquid interface production (a vat with transparent base serves as an oxygen-permeable window, where resin polymerisation is prevented and can flow freely, creating continuous printed material rather than layered material).
3. Binder jetting (BJ): Binding liquid agents and powder print materials are deposited in alternating layers to create the final build, and the binder acts as an adhesive between powder layers. Layer-wise slurry deposition is a variant of BJ that uses a ceramic slip instead of dry powder.

4. Material extrusion (ME): This is also known as fusion deposition modelling, direct ink writing or robocasting, wherein a heated nozzle contains a thermoplastic filament that is melted into an ink and deposited in layers to generate the 3D object. The fabrication of LSCs via ME is achieved by using a ceramic slurry—composed of chemically or heat-bonded ceramic particles—as the ink material.
5. Powder bed fusion (PBF): In this process, a powdered material is selectively melted and fused via laser or electron beams to fabricate the final product. This method can be further subdivided into the following: selective laser sintering, selective laser melting and electron beam Melting. This method has not been successful in fabricating LSC restorations, due to the laser-induced cracks that result from drastic temperature fluctuations.
6. Sheet lamination (SL): In this process, multiple layered sheets of the build are superimposed, laminated and then cut into the final shape using lasers or CNC milling devices.
7. Direct energy deposition (DED): Deposited materials are concurrently melted and fused via focused thermal energy into their final morphologies. Based on the type of thermal energy employed (focused electron beam or focused laser), this method is further divided into laser engineering net shape or electron beam additive manufacturing, respectively.

In general, dental 3D printers function within an XYZ axis system; the X-, and Y-axes control the horizontal movement of the build platform, while the Z-axis controls the vertical movement of the applied nozzle; hence, the latter determines the layer's thickness. The additive manufacturing of LSCs is in its nascent phase, as the unique composition of the ceramics and their heat sensitivity permit them to be fabricated with MJ, VP, BJ, MJ, PBF and DED technologies only [57,60,61].

In order to incorporate LSC material within the feedstock supply, a ceramic powder must be first obtained through calcination or ball milling; subsequently, the powder is mixed with binders/additives into a ceramic slurry that is fed as a printing ink into the manufacturing device and that forms the shaped ceramic with the desired anatomy, i.e., a green body. Upon debinding, the binder burns out and the green body is consolidated into a brown body; the latter is heated in a furnace to promote the complete crystallisation of the ceramic microstructure and achieve a densely sintered body [62]. AM has proven its significant potential in fabricating LSC crowns of high density, thereby yielding improved biaxial flexural strength and reliability as well as fracture toughness and hardness values comparable to those of LSC fabricated via traditional heat pressing methods [63]. Furthermore, recent research data regarding additively manufactured glass products have demonstrated promising efficiency in printing multi-material, multi-scale, and multi-functional glass products, and these could be suggested as the research trends for the 3D printing of LSC restorations in the future [64]. The surface accuracy and internal fit of additive manufacturing-fabricated LSCs is impacted by the print material composition and thickness of the print layers. Nonetheless, the layering in additive manufacturing could result in staircase morphologies that alter the surface texture, hence dictating the need for further finishing and polishing. Unfortunately, the inherent porosities of restorations and the prolonged durations of drying, de-binding and sintering have not been resolved and diminish the appeal of fabricating LSC restorations with additive manufacturing [4,55,56,60,65].

6. Properties

6.1. Biocompatibility

Broadly speaking, LSCs are considered to be among the most biocompatible biomaterials in dentistry based on their high resistance to structural degradation in erosive and corrosive environments. To date, there is an absence of clinical reports of allergic reactions or long-term adverse biological effects of LSCs on tooth structure or surrounding soft tissues [66–70]. ZLS have been deemed biocompatible by the North American Science Associates standards of cytotoxicity, genotoxicity and systemic toxicity [71]. Polished ZLS surfaces present a more homogenous topography in comparison with glazed surfaces, thereby inciting less biofilm accumulation and indicating the promising potential of the former for implant-supported restorations with subgingival margins [72]. Furthermore,

polished ZLS surfaces reveal lower bacterial adhesion and plaque formation than polished LDS ceramics do [73]. Data regarding ZLS biocompatibility in terms of cellular adhesion are scarce; ZLS has been shown to yield lower human periodontal ligament stem cell adhesion than LDS has [74], and lower human gingival fibroblast proliferation than yttrium-stabilised tetragonal zirconia has [75]. Unfortunately, to date, in vitro studies evaluating the ALDs' biocompatibility and cytotoxicity are non-existent, excluding manufacturer-supplied safety data sheets.

6.2. Mechanical Properties

In general, the brittle nature of LSCs provides high resistance to compressive stresses and poor resistance to tensile/shear stresses, and the increase in crystalline content is accompanied by an increase in strength and fracture toughness [38,76]. The hardness of LSCs is higher than that of the tooth structure; hence, it may be a cause of detrimental wear in contrast to resin composite restorations [77–80]. In comparison with leucite reinforced glass-ceramics, LSCs demonstrate superior mechanical properties, allowing them to be applied in high-occlusal-stress-bearing areas [76,81,82]. Studies regarding ZLS restorations have reported high fracture resistance surpassing masticatory occlusal forces, feldspathic ceramics, polymer-infiltrated ceramic networks (PICNs) and bilayered ceramic-veneered zirconia restorations [83–85]. Moreover, ZLS yield adequate flexural strength and fracture toughness values comparable to those of LDS and higher than those of feldspathic ceramics and PICNs [5,22,83]. Wear rates of ZLS (Celtra Duo, Denstply Sirona, Salzburg, Austria) have been shown to not be statistically different from those of dental enamel after artificially induced chewing cycles; nonetheless, the reduced wear rate of fully crystallised ZLS has been noted upon glaze firing [86]. ZLS have demonstrated exceptionally low reliability (i.e., a low Weibull modulus), implying the presence of widely distributed material-dependent strength-limiting defects within their microstructure, ostensibly a result of a thermal mismatch between glass and crystalline phases [22]. Regarding ALDs, some studies have reported similar mechanical strengths to those of LDS and inferior mechanical strengths compared with those of ZLS and zirconia [87,88], while others have reported on the inferior mechanical performance of ALDs compared with that of ZLS or LDS [89,90]. Nonetheless, despite their high crystalline content, ALDs have low fracture toughness [4,5] which is attributed to their nano-scale crystal sizes. In terms of marginal adaptation and the trueness of internal fit, both the ZLS and ALD materials have demonstrated acceptable accuracy and internal adaptation within the required clinical values, and thus have proven to be comparable to those of LDS materials [91–95].

6.3. Optical Properties

The chemical composition, crystalline type and crystalline phase of LSCs have been shown to influence their optical properties, e.g., increased crystalline density decreases light transmission and thereby increases opacity. Furthermore, greater translucency is found in LSCs with smaller crystals and when similar refractive indices exist between glass and crystalline phases [96]. The type and shade of cementing agent, surface treatments, substrate thickness, surface texture and ageing all play a crucial role in the final colour of a restoration [97–100]. LSCs are accessible in a wide range of shades and translucencies; shades are regulated in the manufacturing process by incorporating pigments within the glass matrix, while translucency is regulated via the nano-scaling of crystals [7]. Most products are available in four translucency levels: high translucency (HT), medium translucency (MT), low translucency (LT) and high opacity (HO). Partially crystallised LSC HT blocks contain numerous large-size lithium metasilicate crystals while LT blocks comprise an abundance of smaller crystals [101]. Studies have reported that ZLS restorations demonstrate higher translucency than RNCs, PICNs, feldspathic ceramics, LDS and monolithic zirconia [12,101–103], which is attributed to the smaller silicate crystals and thereby the higher glassy matrix percentage. Conversely, other studies [104] have stated that ZLS exhibit lower translucency and higher opalescence in comparison with LDS and

resin-matrix ceramics, which could be explained by the higher amount of oxides in the former. The translucency of ALD materials is equivalent to that of LDS and ZLS, and is significantly impacted by ageing, glaze treatments and the colour of the underlying substrate [88,105,106].

7. Surface Treatments of LSCs

Mechanical, optical and topographical characteristics of LSC restorations depend on the conditioning treatments applied to the external or internal (intaglio) surfaces.

7.1. Intaglio Surface Treatments

LSC intaglio surfaces must be roughened to amplify the surface area, thereby facilitating luting cement retention and optimising the strength of the bond to the tooth substrate. Nonetheless, extensive alterations to the internal surfaces could be damaging, as they lead to unfavourable glassy matrix removal and grain pull-out, causing adverse volumetric loss that could weaken the LSC [107]. Various chemical, mechanical and chemo-mechanical approaches have been employed to increase the micromechanical retention of LSC substrates.

7.1.1. Mechanical Surface Treatments

- Airborne particle abrasion: Sandblasting with alumina oxide or silica oxide particles creates surface alterations that are determined by the size, hardness, pressure, incident angle and velocity of abrading particles and the distance between the substrate and sandblasting nozzle. Since sharp edges of alumina particles chip away weaker glassy phases creating microcracks, this method could have a degrading impact on LSCs with high glass contents [108,109].
- Laser irradiation: Heat introduction by a laser creates conchoidal (scalloped) defects within LSC surfaces, promoting the micromechanical retention needed for bonding. Erbium: yttrium aluminium garnet laser is commonly employed [110,111], as is CO₂ laser, to treat LSC surfaces, owing to their complete absorption of CO₂ wavelengths [112]. Recently, femtosecond laser treatments have been explored to treat LSC surfaces, wherein ultrashort optical pulses are generated per femtosecond, producing micro-retentive topographical changes [113].

7.1.2. Chemical Surface Treatments

- Hydrofluoric acid etching: The etching of LSC restorations is most frequently performed using buffered hydrofluoric acid (HF), since the unbuffered version of HF is highly caustic; most HF etching products offered in the dental market are buffered down to 5% or 10% concentrations through the addition of an ammonium fluoride (NH₄F) buffering agent. HF reacts with silica in the glassy matrix, yielding a tetrafluorosilane compound (SiF₄), succeeded by a hexafluorosilicate complex ([SiF₆]^{−2}) and subsequently soluble hydrofluorosilicic acid (H₂[SiF₆]) that is washed away along with the glassy matrix, hence exposing the underlying crystalline network (Figure 9) and providing the retention needed for LSC cementation [69,107,114,115].

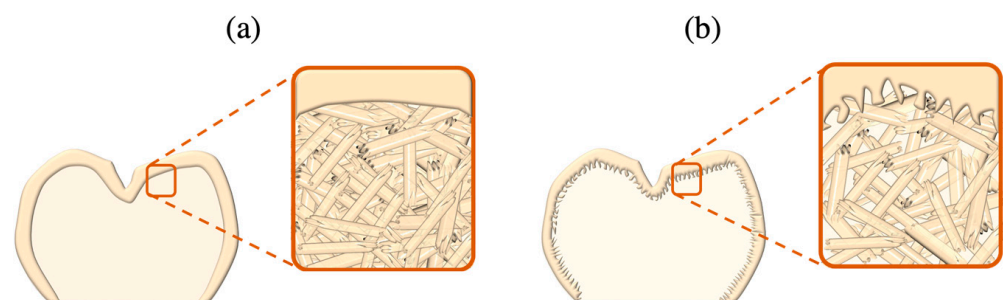
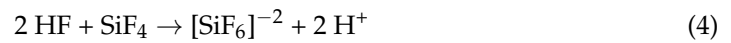
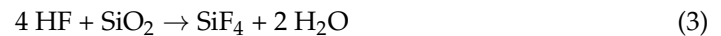


Figure 9. Schematic depiction of LSCs' crystalline structure (a) before and (b) after etching with HF.



X-ray photoelectron spectroscopy (XPS) of superficial atomic layers of etched LSC nano-surfaces (≤ 4 nm) [116] has verified that the HF mechanism of action is actually two-fold; it causes the dissolution of the glassy matrix, and alters the chemical composition of LSCs at a nano-level. LSCs with higher crystalline densities demonstrate lower HF-induced SiO_2 dissolution, as evident from the percentage of SiO_2 remaining in LSC surfaces post-etching; 18.3% SiO_2 was found in IPS e.max CAD (Ivoclar Vivadent, Schaan, Liechtenstein) and 9.1% was found in Celtra Duo (Dentsply Sirona, Salzburg, Austria) [116]. Conversely, the complete dissolution of SiO_2 glass has been seen in etched VITA Suprinity (VITA Zahnfabrik, Bad Säckingen, Germany) and n!ce (Straumann, Basel Switzerland) nano-surfaces [116]. The microscopic evaluation of etched LSC surfaces has revealed elongated crystals distributed among shallow irregularities (Figure 10), in contrast to etched leucite ceramics surfaces that display a characteristic honeycomb-like appearance [114].

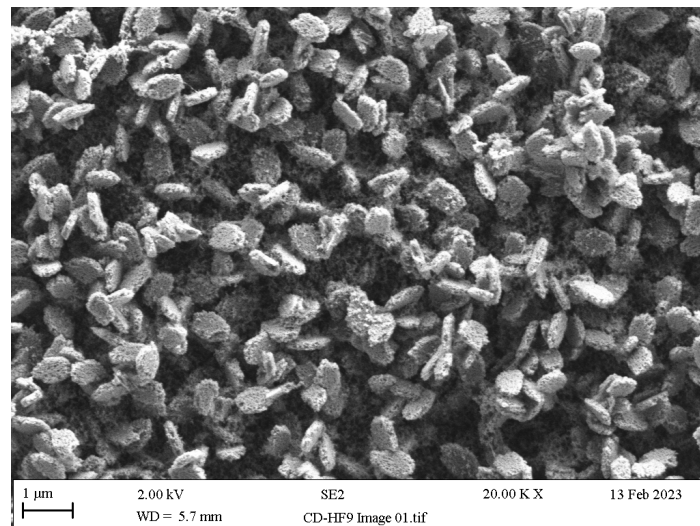


Figure 10. FE-SEM image ($\times 20,000$) of an LSC (Celtra Duo, Dentsply Sirona, Salzburg, Austria) following etching with 9% hydrofluoric acid for 30 s.

The differences between etching patterns are caused by lithium disilicate crystals' greater resistance to HF dissolution compared with that of SiO_2 as twice the HF concentration is needed to dissolve a single lithium disilicate molecule.



Variations in the Li content (atomic%) of nano-layers post-etching are explained by the differing Li:Si ratios in LSCs; a low ratio indicates minimal Li within the glassy matrix, such as in IPS e.max CAD (1:5.75) and in n!ce (1:5.49), whereas a higher ratio implies a lithium-rich glassy matrix, such as in Celtra Duo (1:1.84) and VITA Suprinity (1:2.41) [113]. Many different LSC etching protocols have been investigated in the literature, exploring the effect of etching durations as well as etchant concentration [98,117–126]. In general, etching LSCs had a negative impact on their flexural strength [98,119,120,127]. Moreover, etching with pre-heated HF (50–70 °C) yielded higher bond strengths compared with etching with room-temperature HF [124–126].

- Acid etching with HF substitutes: Owing to the toxic and corrosive potential of HF as a result of its low dissociation constant, it can easily penetrate dermal, epidermal and mucosal tissues entering into the blood stream; however, its slow interaction with nerve endings delays the burning sensation. Hence, HF must be handled with utmost caution in extra-oral conditions, only with adequate ventilation and protective gear [107,128]. Attempts in minimising occupational hazards with HF have led to the exploration of alternative etching modalities with agents of reduced acidic capacities:
 1. Phosphoric acid: Theoretically, etching with phosphoric acid (35–40%) should create LSC morphological modifications; however, microscopic evaluations reveal surfaces minimally altered by phosphoric acid post-etching in comparison with the use of HF and a weaker bond strength [107,129].
 2. Acidulated phosphate fluoride (APF): This is composed of 1.23% fluoride ions derived from sodium fluoride and hydrofluoric acid that become acidified through the addition of phosphoric acid. APF has proven to be a more efficient etchant for leucite-based ceramics than for LDS, due to the faster crystalline dissolution rate in the former [130], with greater bond strengths reported upon longer APF etching durations [107].
 3. Ammonium bifluoride (ABF): Herein, a linear etching pattern is formed due to the targeted action of ABF on grain boundaries and pre-existing cracks within LSCs, reacting with the silica matrix and generating silicon tetrafluoride and ammonium fluoride:



As ABF is less toxic than HF, longer etching times are required to create etching patterns similar to those of HF of similar concentrations. While etching with ABF results in adequate bonding strengths, it is mainly used as an intermediate for fabricating HF [107,131].

4. Ammonium polyfluoride (AP): This is provided within the composition of self-etching ceramic primers (SEP), serves as a silane coupling agent stabiliser and, despite its notably low acidity, has been shown to create sufficient micro-retentive etching patterns in LSCs [132,133] (Figure 11) and reliable adhesion to the tooth substrate [134,135].

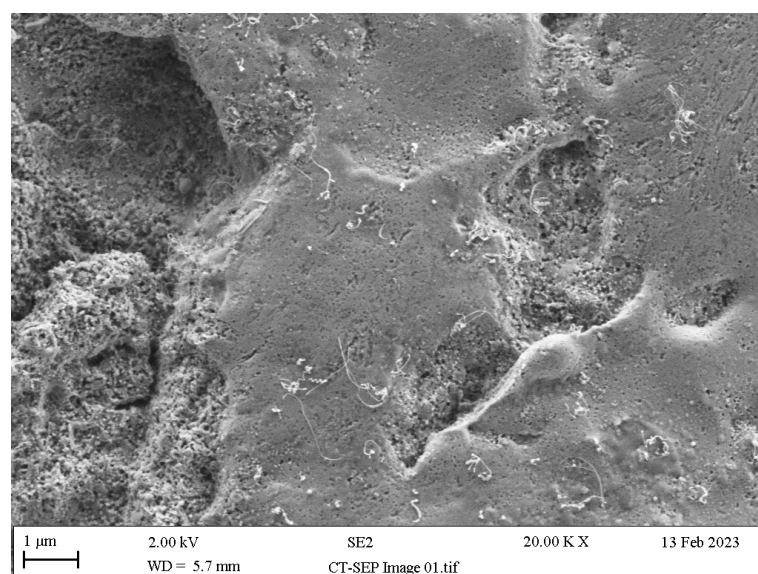


Figure 11. FE-SEM image ($\times 20,000$) of an LSC (Cerec Tessera, Dentsply Sirona, Salzburg, Austria) following etching with a self-etch primer (Monobond Etch & Prime, Ivoclar Vivadent, Schaan, Liechtenstein) under 20 s of active application with a microbrush and then 40 s of passive application.

- Acid neutralisation: Alkaline agents such as calcium gluconate, sodium bicarbonate and calcium carbonate have been used to neutralise the acidity of LSC surfaces caused by HF residues through an acid–base reaction that produces sodium fluoride and calcium fluoride salts and that arrests further etching by HF residues by generating adverse topographical changes (Figure 12) [136–141].

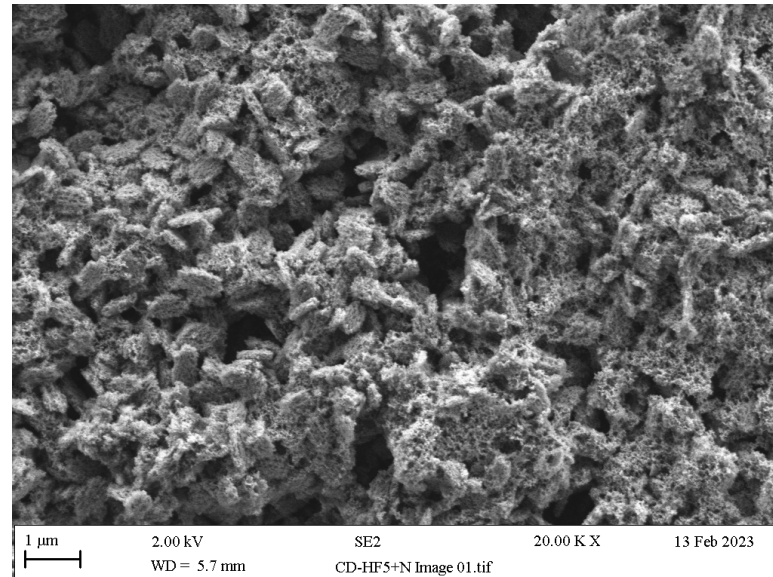
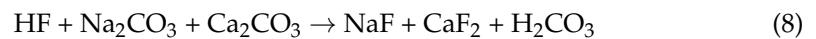


Figure 12. FE-SEM image ($\times 20,000$) of LSC (Celtra Duo, Dentsply Sirona, Salzburg, Austria) after etching with 5% hydrofluoric acid for 30 s and immersion in a neutralising solution for 1 min.

There is contradicting evidence in the literature concerning the impact of acid neutralisation on mechanical and optical traits of ceramics and the strength of their bonding to resin cements. Several studies have observed that neutralising etched ceramic surfaces improves their wettability [89,142] and bond strengths [136,143], while others [140,144] have refuted this observation, claiming that precipitated salts interfere with adequate resin cement penetration and subsequent bonding.

- Salinisation: Silanes comprise a γ -methacryloxypropyltrimethoxysilane molecule that enables bonding between LSC and resin surfaces via its bifunctional monomers; the alkoxy group (methacryloxy, Si-O-CH₃) reacts with the LSCs hydroxyl group (-OH), forming silanol (Si-OH), and, on the silane monomer end, a methacrylate group (C=C) reacts with the organic-matrix monomers of the resin, resulting in a bridging siloxane compound (-Si-O-Si-O-) (Figure 13) that improves LSC wettability and resin penetration [107,109,145]. To achieve the optimal bonding effects of a silane coating, LSCs must be pre-treated, e.g., etched, to increase their roughness [107].
- Plasma treatment: When low-temperature atmospheric-pressure plasma is applied to LSCs, it acts at a molecular level without violating bulk integrity, thereby decontaminating LSCs and increasing their surface energy. Moreover, the dry conditions in which plasma treatment is carried out eliminate the risk of strength-limiting hydrolytic damage, yielding sufficient bond strength values for LSCs bonding to resin cements [146–148].
- 10-methacryloyloxydecyl-dihydrogenphosphate application (10-MDP): 10-MDP is a phosphate ester monomer found in primers as well as resin cements that can chemically react with zirconia by forming a bond with its hydroxyl groups. It has displayed promising bonding performance when used following the silanisation of HF-etched ZLS surfaces [149,150].

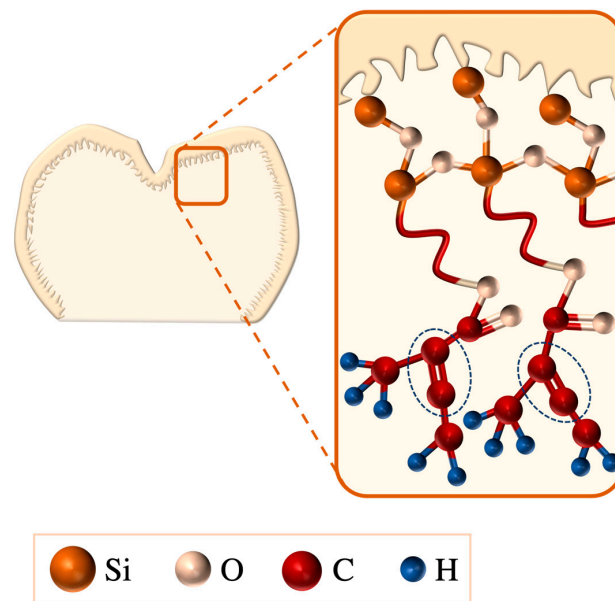


Figure 13. Depiction of the formation of the bridging siloxane compound ($-\text{Si}-\text{O}-\text{Si}-\text{O}-$) as a result of chemical interactions between the silane coupling agent and the etched silicate surfaces. The methacrylate group ($\text{C}=\text{C}$) at the monomer end of the silane coupling agent reacts with the luting agent's organic matrix monomers via the breaking of its double bonds (dashed blue circle). Modified from Benetti et al. [145].

7.1.3. Chemo-Mechanical Surface Treatments

LSC silanisation is facilitated via tribochemical silica-coating, “silicatisation”, through a three-fold mechanism: Al_2O_3 particle airborne abrasion, silica-coated Al_2O_3 particle airborne abrasion and silanisation (Figure 14) [151–154]. Upon contact with LSC surfaces, the kinetic energy of silica-coated Al_2O_3 particles is transferred into thermal energy, thereby melting the silica coating and fusing the former with the LSC surface, creating surfaces that are susceptible for silane chemical interactions and, consequently, improving the strength of bonding to the resin luting agents.

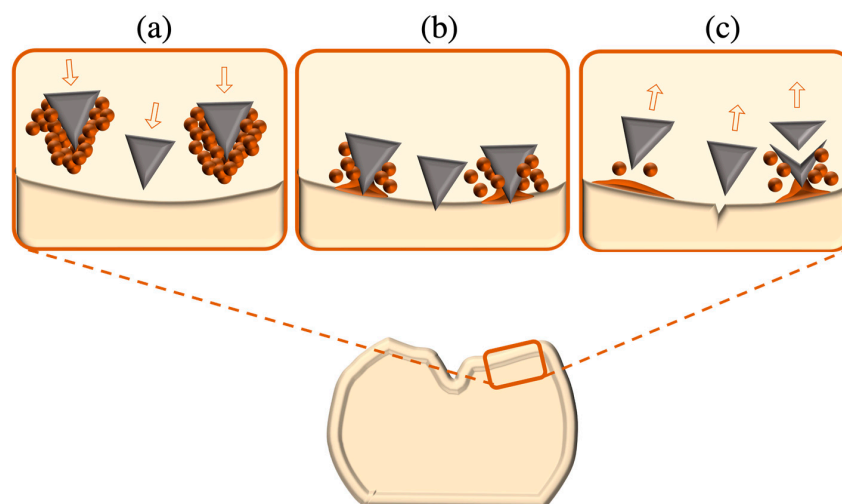


Figure 14. Schematic representation of tribochemical silica coating: (a) Silica (orange)-coated alumina particles (grey) approaching zirconia surfaces. (b) Upon contact with zirconia surfaces, alumina particles' kinetic energy is converted into thermal energy that melts and fuses the silica coating with the zirconia substrate. (c) Most alumina particles are removed completely (left); however, some alumina fragments and unfused silica particles remain (right). Modified from Nagaoka et al. [154].

7.2. External Surface Treatments

It is necessary to implement adequate intra-oral finishing and polishing regimens after intra-oral adjustments are made to LSCs to yield a degree of clinically acceptable surface smoothness [155,156]. Finishing and polishing can be executed lab-side or chairside and the efficacy depends on various parameters such as the abrasive particle size, hardness and shape, applied velocity and pressure, and the LSCs hardness and microstructure. The glazing of LSCs can be accomplished by over-glazing, in which low-fusing glass coating is applied and fired at lower temperatures ($\sim 700^\circ\text{C}$) or via auto-glazing (self-glazing), where a superficial layer of unfilled glass is created upon heating LSCs at a maximum temperature ($\sim 940^\circ\text{C}$) [157]. Glazing pastes, powder–liquid mixtures or sprays are commonly employed in the over-glazing method, all of which comprise a wide range of chemical compositions, some with added pigments or fluorescent agents, applied before the crystallisation of LSC restorations to facilitate simultaneous glazing and crystallisation [158]. Firing and cooling protocols of LSCs also play a significant role in their optical and mechanical performance, as altering the temperature gradients gives rise to residual stresses within the surface and bulk of LSC structures [159].

8. Discussion and Conclusions

In terms of LSC restoration longevity, success rate is a measure of their endurance in situ without the need for any interventions, survival rate is a measure of on-site permanence despite the presence of clinically acceptable complications that may or may not involve further amendments and failure rate is a measure of the technical, biological or aesthetic complications that dictate the replacement of the restoration (e.g., fracture, marginal discrepancy, debonding and discolouration) [160]. Multiple long-term studies have confirmed the high success rate of lithium silicate ceramic restorations [161–167]; however, owing to the recent availability of ZLS and ALD materials in the dental market, there is a lack of long-term systematic data in terms of clinical longevity. Unfired fully crystallised ZLS crowns (Celtra Duo, Dentsply Sirona, Salzburg, Austria) revealed high fracture rates (26%) after one year of clinical function [168], whereas when the same material was exposed to glaze firing, it exhibited a high success rate (98%) after 3 years [169]. Conversely, others [170] reported similar failure rates in unfired and fired ZLS materials after one year of clinical use. Moreover, a 5-year prospective clinical trial of ZLS partial crowns (VITA Suprinity, VITA Zahnfabrik, Bad Säckingen, Germany) showed a success rate of 80% and a 91% survival rate [171]. In general, failure rates of chairside-fabricated ZLS crowns within the first 3 years are comparable to those of lithium disilicate materials with similar clinical durations [172]. In terms of pressable ZLS, the 2-year clinical performance of implant- and tooth-supported three-unit FPD's revealed that complications were mainly due to shade mismatches (7%) and less likely to be mechanical failures (1%) [173]. Limited in vitro studies have investigated the longevity of ALD restorations; a clinical study followed the one-year clinical performance of restorations fabricated from Cerec Tessera (Dentsply Sirona, Salzburg, Austria) and reported a 100% success rate [174]. On the other hand, others have observed the clinical survival of implant-supported monolithic crowns fabricated from n/ce (Straumann, Basel Switzerland) after 33 months and reported a 80.2% success rate. Nevertheless, similar outcomes have been reported for predrilled blocks compared with those of blocks that were manually drilled prior to their sintering [175].

The appealing aesthetics and sufficient strength of LSCs have significantly contributed to their popularity in both the material development sector as well as the clinical application sector. Nonetheless, certain material limitations remain, considering that the mechanical requirements of LSC dental materials still cause them to be inadequate in delivering the strength needs of multiunit prostheses within the molar region [176]. Recently, in vitro experimentations of LSCs have explored the effects of the incorporation of lithium tantalate (LiTaO_3) and lithium niobate (LiNbO_3) precipitations within the crystalline phase composition [8–10] on the radiopacity and hardness, wherein authors concluded positive findings. Furthermore, novel LSC coatings such as DCMHotbond that are applied in thin layers

(<20 µm) on the zirconia fitting surface permitting HF etching and subsequent salinisation should, in theory, yield higher bond strengths. However, the technical sensitivity of this approach and concerns about the thickness and durability of the coating layer have not yet been resolved [11–13].

The improvement of LSCs in terms of dentistry via 3D printing should focus on optimising material composition and printability, refining the surface finish and detail, and enabling customisation for patient-specific needs. Enhancements in additive manufacturing could be tailored to focus on mechanical properties, biocompatibility and longevity. Furthermore, the long-term cost-effectiveness and scalability of these materials are essential considerations for the wider adoption of 3D-printed LSC restorations.

Author Contributions: Conceptualisation, H.A.-J.; methodology, H.A.-J. and J.H.; software, H.A.-J.; validation, H.A.-J., J.H., N.S. and J.S.; formal analysis, H.A.-J. and J.H.; investigation, H.A.-J.; resources, H.A.-J.; data curation, H.A.-J.; writing—original draft preparation, H.A.-J.; writing—review and editing, H.A.-J., J.H., N.S. and J.S.; visualisation, H.A.-J. and J.H.; supervision, J.H., N.S. and J.S.; project administration, J.S. and N.S.; funding acquisition, H.A.-J. All authors have read and agreed to the published version of the manuscript.

Funding: The first author (HA) was funded by a full time scholarship provided by the Saudi Arabian Cultural Bureau in London, UK. The funder had no role in study design, data collection and analysis, decision to publish, or preparation of the manuscript.

Institutional Review Board Statement: Not applicable.

Informed Consent Statement: Not applicable.

Data Availability Statement: The data presented in this study are available on request from the corresponding author.

Acknowledgments: The authors acknowledge the contribution of Hayley Andrews (Faculty of Science and Engineering, Manchester Metropolitan University) for the experimental work on scanning electron microscopy.

Conflicts of Interest: The authors declare no conflicts of interest.

References

1. Stookey, S. Catalyzed crystallization of glass in theory and practice. *Ind. Eng. Chem.* **1959**, *51*, 805–808. [\[CrossRef\]](#)
2. Beall, G. Design and properties of glass-ceramics. *Ann. Rev. Mater. Sci.* **1992**, *22*, 91–119. [\[CrossRef\]](#)
3. Willard, A.; Chu, T.M.G. The science and application of IPS e. Max dental ceramic. *Kaohsiung J. Med. Sci.* **2018**, *34*, 238–242. [\[CrossRef\]](#) [\[PubMed\]](#)
4. Zhang, Y.; Vardhaman, S.; Rodrigues, C.S.; Lawn, B.R. A Critical Review of Dental Lithia-Based Glass-Ceramics. *J. Dent. Res.* **2023**, *102*, 245–253. [\[CrossRef\]](#) [\[PubMed\]](#)
5. Lubauer, J.; Belli, R.; Peterlik, H.; Hurle, K.; Lohbauer, U. Grasping the Lithium hype: Insights into modern dental Lithium Silicate glass-ceramics. *Dent. Mater.* **2022**, *38*, 318–332. [\[CrossRef\]](#) [\[PubMed\]](#)
6. Zarone, F.; Ruggiero, G.; Leone, R.; Breschi, L.; Leuci, S.; Sorrentino, R. Zirconia-reinforced lithium silicate (ZLS) mechanical and biological properties: A literature review. *J. Dent.* **2021**, *109*, 103661. [\[CrossRef\]](#) [\[PubMed\]](#)
7. Phark, J.H.; Duarte, S., Jr. Microstructural considerations for novel lithium disilicate glass ceramics: A review. *J. Esthet. Restor. Dent.* **2022**, *34*, 92–103. [\[CrossRef\]](#) [\[PubMed\]](#)
8. DeCeanne, A.V.; Fry, A.L.; Wilkinson, C.J.; Dittmer, M.; Ritzberger, C.; Rampf, M.; Mauro, J.C. Experimental analysis and modeling of the Knoop hardness of lithium disilicate glass-ceramics containing lithium tantalate as a secondary phase. *J. Non-Cryst. Solids.* **2022**, *585*, 121540. [\[CrossRef\]](#)
9. Dittmer, M.; Ritzberger, C.; Höland, W.; Rampf, M. Controlled precipitation of lithium disilicate (Li₂Si₂O₅) and lithium niobate (LiNbO₃) or lithium tantalate (LiTaO₃) in glass-ceramics. *J. Eur. Ceram. Soc.* **2018**, *38*, 263–269. [\[CrossRef\]](#)
10. DeCeanne, A.V.; Fry, A.L.; Wilkinson, C.J.; Dittmer, M.; Ritzberger, C.; Rampf, M.; Mauro, J.C. Examining the phase evolution of lithium disilicate glass-ceramics with lithium tantalate as a secondary phase. *J. Am. Ceram. Soc.* **2022**, *105*, 268–278. [\[CrossRef\]](#)
11. Wattanasirmkit, K.; Srimanepong, V.; Kanchanatawewat, K.; Monmaturapoj, N.; Thunyakitpisal, P.; Jinawath, S. Improving shear bond strength between feldspathic porcelain and zirconia substructure with lithium disilicate glass-ceramic liner. *Dent. Mater. J.* **2015**, *34*, 302–309. [\[CrossRef\]](#) [\[PubMed\]](#)
12. Thammajaruk, P.; Buranadham, S.; Guazzato, M.; Swain, M.V. Influence of ceramic-coating techniques on composite-zirconia bonding: Strain energy release rate evaluation. *Dent. Mater.* **2022**, *38*, e31–e42. [\[CrossRef\]](#) [\[PubMed\]](#)

13. Thammajaruk, P.; Buranadham, S.; Thanatvarakorn, O.; Ferrari, M.; Guazzato, M. Influence of glass-ceramic coating on composite zirconia bonding and its characterization. *Dent. Mater.* **2019**, *35*, 105–113. [\[CrossRef\]](#)
14. Manziuc, M.; Kui, A.; Chisnoiu, A.; Labunet, A.; Negucioiu, M.; Ispas, A.; Buduru, S. Zirconia-Reinforced Lithium Silicate Ceramic in Digital Dentistry: A Comprehensive Literature Review of Our Current Understanding. *Medicina* **2023**, *59*, 2135. [\[CrossRef\]](#) [\[PubMed\]](#)
15. Sorrentino, R.; Ruggiero, G.; Di Mauro, M.I.; Breschi, L.; Leuci, S.; Zarone, F. Optical behaviors, surface treatment, adhesion, and clinical indications of zirconia-reinforced lithium silicate (ZLS): A narrative review. *J. Dent.* **2021**, *112*, 103722. [\[CrossRef\]](#) [\[PubMed\]](#)
16. Souza, I.V.; Finck, N.S.; Rodrigues, C.S.; Moraes, R.R. Laboratory processing methods and bonding to glass ceramics: Systematic review. *Int. J. Adhes. Adhes.* **2024**, *129*, 103572. [\[CrossRef\]](#)
17. Sacher, E.; França, R. *Dental Biomaterials*; World Scientific: Singapore, 2018.
18. Ortiz, A.L.; Rodrigues, C.S.; Guiberteau, F.; Zhang, Y. Microstructural development during crystallization firing of a dental-grade nanostructured lithia-zirconia glass-ceramic. *J. Eur. Ceram. Soc.* **2021**, *41*, 5728–5739. [\[CrossRef\]](#)
19. Simba, B.G.; Ribeiro, M.V.; Alves, M.F.R.P.; Vasconcelos Amarante, J.E.; Strecker, K.; dos Santos, C. Effect of the temperature on the mechanical properties and translucency of lithium silicate dental glass-ceramic. *Ceram. Int.* **2021**, *47*, 9933–9940. [\[CrossRef\]](#)
20. França, R. Lithium disilicate-based glass-ceramics. In *Dental Biomaterials*; World Scientific: Singapore, 2019; pp. 173–209.
21. Belli, R.; Wendler, M.; de Ligny, D.; Cicconi, M.R.; Petschelt, A.; Peterlik, H.; Lohbauer, U. Chairside CAD/CAM materials. Part 1: Measurement of elastic constants and microstructural characterization. *Dent. Mater.* **2017**, *33*, 84–98. [\[CrossRef\]](#) [\[PubMed\]](#)
22. Wendler, M.; Belli, R.; Petschelt, A.; Mevec, D.; Harrer, W.; Lube, T.; Danzer, R.; Lohbauer, U. Chairside CAD/CAM materials. Part 2: Flexural strength testing. *Dent. Mater.* **2017**, *33*, 99–109. [\[CrossRef\]](#) [\[PubMed\]](#)
23. Krüger, S.; Deubener, J.; Ritzberger, C.; Höland, W. Nucleation kinetics of lithium metasilicate in ZrO₂-bearing lithium disilicate glasses for dental application. *Int. J. Appl. Glass Sci.* **2013**, *4*, 9–19. [\[CrossRef\]](#)
24. Dentsply Sirona. Scientific Documentation Celtra Duo. 2017. Available online: https://www.dentsplysirona.com/content/dam/master/education/documents/upload/6/67835_Celtra_Duo_Broschyr_LowRes.pdf (accessed on 20 January 2024).
25. von Maltzahn, N.F.; El Meniawy, O.I.; Breitenbuecher, N.; Kohorst, P.; Stiesch, M.; Eisenburger, M. Fracture Strength of Ceramic Posterior Occlusal Veneers for Functional Rehabilitation of an Abrasive Dentition. *Int. J. Prosthodont.* **2018**, *31*, 451–452. [\[CrossRef\]](#) [\[PubMed\]](#)
26. Sieper, K.; Wille, S.; Kern, M. Fracture strength of lithium disilicate crowns compared to polymer-infiltrated ceramic-network and zirconia reinforced lithium silicate crowns. *J. Mech. Behav. Biomed. Mater.* **2017**, *74*, 342–348. [\[CrossRef\]](#) [\[PubMed\]](#)
27. Elsaka, S.E.; Elnaghy, A.M. Mechanical properties of zirconia reinforced lithium silicate glass-ceramic. *Dent. Mater.* **2016**, *32*, 908–914. [\[CrossRef\]](#) [\[PubMed\]](#)
28. Al-Johani, H.; Haider, J.; Silikas, N.; Satterthwaite, J. Effect of repeated firing on the topographical, optical, and mechanical properties of fully crystallized lithium silicate-based ceramics. *J. Prosthet. Dent.* **2024**, *131*, 741.e1–741.e11. [\[CrossRef\]](#)
29. Ramos Nde, C.; Campos, T.M.; Paz, I.S.; Machado, J.P.; Bottino, M.A.; Cesar, P.F.; de Melo, R.M. Microstructure characterization and SCG of newly engineered dental ceramics. *Dent. Mater.* **2016**, *32*, 870–878. [\[CrossRef\]](#) [\[PubMed\]](#)
30. Monmaturapoj, N.; Lawita, P.; Thepsuwan, W. Characterisation and properties of lithium disilicate glass ceramics in the SiO₂-Li₂OK₂O-Al₂O₃ system for dental applications. *Adv. Mater. Sci. Eng.* **2013**, *2013*, 763838. [\[CrossRef\]](#)
31. Hurlle, K.; Lubauer, J.; Belli, R.; Lohbauer, U. On the assignment of quartz-like LiAlSi₂O₆—SiO₂ solid solutions in dental lithium silicate glass-ceramics: Virgilite, high quartz, low quartz or stuffed quartz derivatives? *Dent. Mater.* **2022**, *38*, 1558–1563. [\[CrossRef\]](#) [\[PubMed\]](#)
32. Montazerian, M.; Dutra Zanotto, E. History and trends of bioactive glass-ceramics. *J. Biomed. Mater. Res. A* **2016**, *104*, 1231–1249. [\[CrossRef\]](#) [\[PubMed\]](#)
33. Wang, F.; Li, K.; Ning, C. Sintering properties of sol-gel derived lithium disilicate glass ceramics. *J. Solgel Sci. Technol.* **2018**, *87*, 372–379. [\[CrossRef\]](#)
34. Fu, L.; Engqvist, H.; Xia, W. Glass-ceramics in dentistry: A review. *Materials* **2020**, *13*, 1049. [\[CrossRef\]](#) [\[PubMed\]](#)
35. Liu, X.; Yao, X.; Zhang, R.; Sun, L.; Zhang, Z.; Zhao, Y.; Zhang, T.; Yan, J.; Zhang, Y.; Wu, X.; et al. Recent advances in glass-ceramics: Performance and toughening mechanisms in restorative dentistry. *J. Biomed. Mater. Res. B Appl. Biomater.* **2023**, *112*, e35334. [\[CrossRef\]](#) [\[PubMed\]](#)
36. Khalkhali, Z.; Yekta, B.E.; Marghussian, V. Preparation of lithium disilicate glass-ceramics as dental bridge material. *J. Ceram. Sci. Technol.* **2014**, *5*, 39–44.
37. Li, K.; Kou, H.; Ning, C. Sintering and mechanical properties of lithium disilicate glass-ceramics prepared by sol-gel method. *J. Non-Cryst. Solids.* **2021**, *552*, 120443. [\[CrossRef\]](#)
38. Sakaguchi, R.L.; Ferracane, J.; Powers, J.M. *Craig's Restorative Dental Materials-e-Book*, 14th ed.; Elsevier Health Sciences: Amsterdam, The Netherlands, 2019.
39. Ghazy, M.H.; Madina, M.M.; Aboushelib, M.N. Influence of fabrication techniques and artificial aging on the fracture resistance of different cantilever zirconia fixed dental prostheses. *J. Adhes. Dent.* **2012**, *14*, 161–166. [\[PubMed\]](#)
40. Gonzaga, C.C.; Cesar, P.F.; Miranda, W.G.; Yoshimura, H.N. Slow crack growth and reliability of dental ceramics. *Dent. Mater.* **2011**, *27*, 394–406. [\[CrossRef\]](#) [\[PubMed\]](#)

41. Rösler, J.; Harders, H.; Bäker, M. *Mechanical Behaviour of Engineering Materials: Metals, Ceramics, Polymers, and Composites*; Springer Science & Business Media: Berlin/Heidelberg, Germany, 2007.
42. Shenoy, A.; Shenoy, N. Dental ceramics: An update. *J. Conserv. Dent.* **2010**, *13*, 195. [[CrossRef](#)] [[PubMed](#)]
43. Ruales-Carrera, E.; Dal Bó, M.; Fernandes das Neves, W.; Fredel, M.C.; Maziero Volpato, C.A.; Hotza, D. Chemical tempering of feldspathic porcelain for dentistry applications: A review. *Open Ceram.* **2022**, *9*, 100201. [[CrossRef](#)]
44. Chen, X.; Bei, G. Toughening Mechanisms in Nanolayered MAX Phase Ceramics—A Review. *Materials* **2017**, *10*, 366. [[CrossRef](#)] [[PubMed](#)]
45. Li, D.; Chen, Z.X.; Zhang, Y.M.; Li, X.C.; Meng, M.; He, L.; Zhang, Z.Z. Improved reliability of mechanical behavior for a thermal tempered lithium disilicate glass-ceramic by regulating the cooling rate. *J. Mech. Behav. Biomed. Mater.* **2021**, *114*, 104191. [[CrossRef](#)] [[PubMed](#)]
46. Shannon, R.D. Revised effective ionic radii and systematic studies of interatomic distances in halides and chalcogenides. *Acta Cryst. A* **1976**, *32*, 751–767. [[CrossRef](#)]
47. Li, X.C.; Meng, M.; Li, D.; Wei, R.; He, L.; Zhang, S.F. Strengthening and toughening of a multi-component lithium disilicate glass-ceramic by ion-exchange. *J. Eur. Ceram. Soc.* **2020**, *40*, 4635–4646. [[CrossRef](#)]
48. McLaren, E.; Giordano, R. Ceramics overview: Classification by microstructure and processing methods. *Compend. Contin. Educ. Dent.* **2010**, *31*, 682–684.
49. Santos, M.J.; Costa, M.D.; Rubo, J.H.; Pegoraro, L.F.; Santos, G.C., Jr. Current all-ceramic systems in dentistry: A review. *Compend. Contin. Educ. Dent.* **2015**, *36*, 31–37. [[PubMed](#)]
50. Miyazaki, T.; Hotta, Y.; Kunii, J.; Kuriyama, S.; Tamaki, Y. A review of dental CAD/CAM: Current status and future perspectives from 20 years of experience. *Dent. Mater. J.* **2009**, *28*, 44–56. [[CrossRef](#)] [[PubMed](#)]
51. Samra, A.P.B.; Morais, E.; Mazur, R.F.; Vieira, S.R.; Rached, R.N. CAD/CAM in dentistry—A critical review. *Rev. Odonto Ciência.* **2016**, *31*, 140–144. [[CrossRef](#)]
52. Miyazaki, T.; Hotta, Y. CAD/CAM systems available for the fabrication of crown and bridge restorations. *Aust. Dent. J.* **2011**, *56* (Suppl. S1), 97–106. [[CrossRef](#)] [[PubMed](#)]
53. Rekow, E.D. Digital dentistry: The new state of the art—Is it disruptive or destructive? *Dent. Mater.* **2020**, *36*, 9–24. [[CrossRef](#)] [[PubMed](#)]
54. Turkyilmaz, I.; Wilkins, G.N. Milling Machines in Dentistry: A Swiftly Evolving Technology. *J. Craniofac. Surg.* **2021**, *32*, 2259–2260. [[CrossRef](#)] [[PubMed](#)]
55. van Noort, R. The future of dental devices is digital. *Dent. Mater.* **2012**, *28*, 3–12. [[CrossRef](#)] [[PubMed](#)]
56. Abduo, J.; Lyons, K.; Bennamoun, M. Trends in computer-aided manufacturing in prosthodontics: A review of the available streams. *Int. J. Dent.* **2014**, *2014*, 783948. [[CrossRef](#)] [[PubMed](#)]
57. Galante, R.; Figueiredo-Pina, C.G.; Serro, A.P. Additive manufacturing of ceramics for dental applications: A review. *Dent. Mater.* **2019**, *35*, 825–846. [[CrossRef](#)] [[PubMed](#)]
58. Al Hamad, K.Q.; Al-Rashdan, B.A.; Ayyad, J.Q.; Al Omrani, L.M.; Sharoh, A.M.; Al Nimri, A.M.; Al-Kaff, F.T. Additive Manufacturing of Dental Ceramics: A Systematic Review and Meta-Analysis. *J. Prosthodont.* **2022**, *31*, e67–e86. [[CrossRef](#)] [[PubMed](#)]
59. Tigmeanu, C.V.; Ardelean, L.C.; Rusu, L.-C.; Negrutiu, M.-L. Additive Manufactured Polymers in Dentistry, Current State-of-the-Art and Future Perspectives-A Review. *Polymers* **2022**, *14*, 3658. [[CrossRef](#)] [[PubMed](#)]
60. Wang, G.; Wang, S.; Dong, X.; Zhang, Y.; Shen, W. Recent progress in additive manufacturing of ceramic dental restorations. *J. Mater. Res Technol.* **2023**, *26*, 1028–1049. [[CrossRef](#)]
61. Marsico, C.; Carpenter, I.; Kutsch, J.; Fehrenbacher, L.; Arola, D. Additive manufacturing of lithium disilicate glass-ceramic by vat polymerization for dental appliances. *Dent. Mater.* **2022**, *38*, 2030–2040. [[CrossRef](#)] [[PubMed](#)]
62. Lakhdar, Y.; Tuck, C.; Binner, J.; Terry, A.; Goodridge, R. Additive manufacturing of advanced ceramic materials. *Prog. Mater. Sci.* **2021**, *116*, 100736. [[CrossRef](#)]
63. Baumgartner, S.; Gmeiner, R.; Schönherr, J.A.; Stampfl, J. Stereolithography-based additive manufacturing of lithium disilicate glass ceramic for dental applications. *Mater. Sci. Eng. C Mater. Biol. Appl.* **2020**, *116*, 111180. [[CrossRef](#)] [[PubMed](#)]
64. Xin, C.; Li, Z.; Hao, L.; Li, Y. A comprehensive review on additive manufacturing of glass: Recent progress and future outlook. *Mater. Des.* **2023**, *227*, 111736. [[CrossRef](#)]
65. Choi, S.H.; Chan, A.M.M. A virtual prototyping system for rapid product development. *Comput. Aided Des.* **2004**, *36*, 401–412. [[CrossRef](#)]
66. Bergmann, C.; Stumpf, A. *Dental Ceramics: Microstructure, Properties and Degradation*; Springer Science & Business Media: Berlin/Heidelberg, Germany, 2013.
67. Lygre, H. Prosthodontic biomaterials and adverse reactions: A critical review of the clinical and research literature. *Acta Odontol. Scand.* **2002**, *60*, 1–9. [[CrossRef](#)] [[PubMed](#)]
68. Mallineni, S.K.; Nuvvula, S.; Matinlinna, J.P.; Yiu, C.K.; King, N.M. Biocompatibility of various dental materials in contemporary dentistry: A narrative insight. *J. Investig. Clin. Dent.* **2013**, *4*, 9–19. [[CrossRef](#)] [[PubMed](#)]
69. Ho, G.W.; Matinlinna, J.P. Insights on ceramics as dental materials. Part I: Ceramic material types in dentistry. *Silicon* **2011**, *3*, 109–115. [[CrossRef](#)]

70. Roulet, J.; Söderholm, K.; Longmate, J. Effects of treatment and storage conditions on ceramic/composite bond strength. *J. Dent. Res.* **1995**, *74*, 381–387. [CrossRef] [PubMed]
71. Suprinity, V. *Technical and Scientific Documentation*; Vita Zahnfabrik: Bad Säckingen, Germany, 2014.
72. De Luca Pedro, G.; Carvalho Geraldo, A.; Franco Aline, B.; Simone, K.; Avila Gisseli, B.; Dias Sergio, C. Zirconia-reinforced lithium silicate biocompatibility polished in different Stages-An In vitro study. *J. Int. Dent. Med. Res.* **2018**, *11*, 759–764.
73. Abdalla, M.M.; Ali, I.A.; Khan, K.; Mattheos, N.; Murbay, S.; Matinlinna, J.P.; Neelakantan, P. The influence of surface roughening and polishing on microbial biofilm development on different ceramic materials. *J. Prosthodont.* **2021**, *30*, 447–453. [CrossRef]
74. Mavriqi, L.; Valente, F.; Murmura, G.; Sinjari, B.; Macri, M.; Trubiani, O.; Caputi, S.; Traini, T. Lithium disilicate and zirconia reinforced lithium silicate glass-ceramics for CAD/CAM dental restorations: Biocompatibility, mechanical and microstructural properties after crystallization. *J. Dent.* **2022**, *119*, 104054. [CrossRef] [PubMed]
75. Rizo-Gorrita, M.; Luna-Oliva, I.; Serrera-Figallo, M.; Gutiérrez-Pérez, J.L.; Torres-Lagares, D. Comparison of Cytomorphometry and Early Cell Response of Human Gingival Fibroblast (HGFs) between Zirconium and New Zirconia-Reinforced Lithium Silicate Ceramics (ZLS). *Int. J. Mol. Sci.* **2018**, *19*, 2718. [CrossRef] [PubMed]
76. Denry, I.; Holloway, J.A. Ceramics for dental applications: A review. *Materials* **2010**, *3*, 351–368. [CrossRef]
77. Shen, C.; Rawls, H.R.; Esquivel-Upshaw, J.F. *Phillips' Science of Dental Materials*, 13th ed.; Elsevier Health Sciences: Amsterdam, The Netherlands, 2021.
78. Bajraktarova-Valjakova, E.; Korunoska-Stevkovska, V.; Kapusevska, B.; Gigovski, N.; Bajraktarova-Misevska, C.; Grozdanov, A. Contemporary dental ceramic materials, a review: Chemical composition, physical and mechanical properties, indications for use. *Open Access Maced. J. Med. Sci.* **2018**, *6*, 1742. [CrossRef] [PubMed]
79. Mörmann, W.H.; Stawarczyk, B.; Ender, A.; Sener, B.; Attin, T.; Mehl, A. Wear characteristics of current aesthetic dental restorative CAD/CAM materials: Two-body wear, gloss retention, roughness and Martens hardness. *J. Mech. Behav. Biomed. Mater.* **2013**, *20*, 113–125. [CrossRef] [PubMed]
80. Lawson, N.C.; Bansal, R.; Burgess, J.O. Wear, strength, modulus and hardness of CAD/CAM restorative materials. *Dent. Mater.* **2016**, *32*, e275–e283. [CrossRef]
81. Ivoclar Vivadent. Scientific Documentation IPS e.max CAD. Available online: https://www.ivoclar.com/en_li/products/digital-processes/ips-e.max-cad (accessed on 25 January 2024).
82. Ritzberger, C.; Apel, E.; Höland, W.; Peschke, A.; Rheinberger, V.M. Properties and Clinical Application of Three Types of Dental Glass-Ceramics and Ceramics for CAD-CAM Technologies. *Materials* **2010**, *3*, 3700–3713. [CrossRef]
83. Al-Akhali, M.; Chaar, M.S.; Elsayed, A.; Samran, A.; Kern, M. Fracture resistance of ceramic and polymer-based occlusal veneer restorations. *J. Mech. Behav. Biomed. Mater.* **2017**, *74*, 245–250. [CrossRef] [PubMed]
84. Choi, S.; Yoon, H.I.; Park, E.J. Load-bearing capacity of various CAD/CAM monolithic molar crowns under recommended occlusal thickness and reduced occlusal thickness conditions. *J. Adv. Prosthodont.* **2017**, *9*, 423–431. [CrossRef] [PubMed]
85. Hamza, T.A.; Sherif, R.M. Fracture resistance of monolithic glass-ceramics versus bilayered zirconia-based restorations. *J. Prosthodont.* **2019**, *28*, e259–e264. [CrossRef] [PubMed]
86. D'Arcangelo, C.; Vanini, L.; Rondoni, G.D.; De Angelis, F. Wear properties of dental ceramics and porcelains compared with human enamel. *J. Prosthet. Dent.* **2016**, *115*, 350–355. [CrossRef] [PubMed]
87. Al-Haj Husain, N.; Dürr, T.; Özcan, M.; Brägger, U.; Joda, T. Mechanical stability of dental CAD-CAM restoration materials made of monolithic zirconia, lithium disilicate, and lithium disilicate–strengthened aluminosilicate glass-ceramic with and without fatigue conditions. *J. Prosthet. Dent.* **2022**, *128*, 73–78. [CrossRef] [PubMed]
88. Demirel, M.; Diken Türksayar, A.A.; Donmez, M.B. Translucency, color stability, and biaxial flexural strength of advanced lithium disilicate ceramic after coffee thermocycling. *J. Esthet. Restor. Dent.* **2022**, *35*, 390–396. [CrossRef] [PubMed]
89. Al-Johani, H.; Haider, J.; Silikas, N.; Satterthwaite, J. Effect of surface treatments on optical, topographical and mechanical properties of CAD/CAM reinforced lithium silicate glass ceramics. *Dent. Mater.* **2023**, *39*, 779–789. [CrossRef] [PubMed]
90. Freitas, J.S.; Souza, L.F.B.; Pereira, G.K.R.; May, L.G. Surface properties and flexural fatigue strength of an advanced lithium disilicate. *J. Mech. Behav. Biomed. Mater.* **2023**, *147*, 106154. [CrossRef] [PubMed]
91. Preis, V.; Behr, M.; Hahnel, S.; Rosentritt, M. Influence of cementation on in vitro performance, marginal adaptation and fracture resistance of CAD/CAM-fabricated ZLS molar crowns. *Dent. Mater.* **2015**, *31*, 1363–1369. [CrossRef] [PubMed]
92. Demirel, M.; Donmez, M.B. Fabrication trueness and internal fit of different lithium disilicate ceramics according to post-milling firing and material type. *J. Dent.* **2024**, *144*, 104987. [CrossRef] [PubMed]
93. Falahchai, M.; Babaee Hemmati, Y.; Neshandar Asli, H.; Neshandar Asli, M. Marginal adaptation of zirconia-reinforced lithium silicate overlays with different preparation designs. *J. Esthet. Restor. Dent.* **2020**, *32*, 823–830. [CrossRef] [PubMed]
94. Rizk, A.; El-Guindy, J.; Abdou, A.; Ashraf, R.; Kusumasari, C.; Eldin, F.E. Marginal adaptation and fracture resistance of virgilite-based occlusal veneers with varying thickness. *BMC Oral Health* **2024**, *24*, 307. [CrossRef] [PubMed]
95. Ferrini, F.; Paolone, G.; Di Domenico, G.L.; Pagani, N.; Gherlone, E.F. SEM Evaluation of the Marginal Accuracy of Zirconia, Lithium Disilicate, and Composite Single Crowns Created by CAD/CAM Method: Comparative Analysis of Different Materials. *Materials* **2023**, *16*, 2413. [CrossRef] [PubMed]
96. Höland, W.; Beall, G.H. *Glass-Ceramic Technology*; John Wiley & Sons: Hoboken, NJ, USA, 2019.
97. Vafaei, F.; Heidari, B.; Khoshhal, M.; Hooshyarfar, A.; Izadi, M.; Shahbazi, A.; Moghimbeigi, A. Effect of resin cement color on the final color of lithium disilicate all-ceramic restorations. *J. Dent.* **2018**, *15*, 143.

98. Kurtulmus-Yilmaz, S.; Cengiz, E.; Ongun, S.; Karakaya, I. The effect of surface treatments on the mechanical and optical behaviors of CAD/CAM restorative materials. *J. Prosthodont.* **2019**, *28*, e496–e503. [\[CrossRef\]](#) [\[PubMed\]](#)
99. Vasiliu, R.-D.; Porojan, S.D.; Birdeanu, M.I.; Porojan, L. Effect of Thermocycling, Surface Treatments and Microstructure on the Optical Properties and Roughness of CAD-CAM and Heat-Pressed Glass Ceramics. *Materials* **2020**, *13*, 381. [\[CrossRef\]](#) [\[PubMed\]](#)
100. Della Bona, A.; Nogueira, A.D.; Pecho, O.E. Optical properties of CAD–CAM ceramic systems. *J. Dent.* **2014**, *42*, 1202–1209. [\[CrossRef\]](#) [\[PubMed\]](#)
101. Awad, D.; Stawarczyk, B.; Liebermann, A.; Ilie, N. Translucency of esthetic dental restorative CAD/CAM materials and composite resins with respect to thickness and surface roughness. *J. Prosthet. Dent.* **2015**, *113*, 534–540. [\[CrossRef\]](#) [\[PubMed\]](#)
102. Subaşı, M.G.; Alp, G.; Johnston, W.M.; Yilmaz, B. Effect of thickness on optical properties of monolithic CAD-CAM ceramics. *J. Dent.* **2018**, *71*, 38–42. [\[CrossRef\]](#) [\[PubMed\]](#)
103. Bacchi, A.; Boccardi, S.; Alessandretti, R.; Pereira, G.K.R. Substrate masking ability of bilayer and monolithic ceramics used for complete crowns and the effect of association with an opaque resin-based luting agent. *J. Prosthodont. Res.* **2019**, *63*, 321–326. [\[CrossRef\]](#) [\[PubMed\]](#)
104. Gunal, B.; Ulusoy, M.M. Optical properties of contemporary monolithic CAD-CAM restorative materials at different thicknesses. *J. Esthet. Restor. Dent.* **2018**, *30*, 434–441. [\[CrossRef\]](#) [\[PubMed\]](#)
105. Blackburn, J.; Jackson, T.; Cook, R.; Sulaiman, T.A. Optical properties of a novel glass–ceramic restorative material. *J. Esthet. Restor. Dent.* **2021**, *33*, 1160–1165. [\[CrossRef\]](#) [\[PubMed\]](#)
106. Liebermann, A.; Mandl, A.; Eichberger, M.; Stawarczyk, B. Impact of resin composite cement on color of computer-aided design/computer-aided manufacturing ceramics. *J. Esthet. Restor. Dent.* **2021**, *33*, 786–794. [\[CrossRef\]](#) [\[PubMed\]](#)
107. Ho, G.W.; Matinlinna, J.P. Insights on ceramics as dental materials. Part II: Chemical surface treatments. *Silicon* **2011**, *3*, 117–123. [\[CrossRef\]](#)
108. Aswal, G.; Nair, C. Effects of various parameters of alumina air abrasion on the mechanical properties of low-fusing feldspathic porcelain laminate material. *S. Afr. Dent. J.* **2015**, *70*, 150–155.
109. Amorim, R.; Vermudt, A.; Pereira, J.R.; Pamato, S. The surface treatment of dental ceramics: An overview. *J. Res. Dent.* **2018**, *6*, 4. [\[CrossRef\]](#)
110. Aladağ, S.Ü.; Ayaz, E.A. Repair bond strength of different CAD-CAM ceramics after various surface treatments combined with laser irradiation. *Lasers Med. Sci.* **2023**, *38*, 51. [\[CrossRef\]](#) [\[PubMed\]](#)
111. Altan, B.; Cinar, S.; Tuncelli, B. Evaluation of shear bond strength of zirconia-based monolithic CAD-CAM materials to resin cement after different surface treatments. *Niger. J. Clin. Pract.* **2019**, *22*, 1475–1482. [\[CrossRef\]](#) [\[PubMed\]](#)
112. Souza, J.C.M.; Raffaele-Esposito, A.; Carvalho, O.; Silva, F.; Özcan, M.; Henriques, B. Surface modification of zirconia or lithium disilicate-reinforced glass ceramic by laser texturing to increase the adhesion of prosthetic surfaces to resin cements: An integrative review. *Clin. Oral Investig.* **2023**, *27*, 3331–3345. [\[CrossRef\]](#) [\[PubMed\]](#)
113. Inokoshi, M.; Yoshihara, K.; Kakehata, M.; Yashiro, H.; Nagaoka, N.; Tonprasong, W.; Xu, K.; Minakuchi, S. Preliminary Study on the Optimization of Femtosecond Laser Treatment on the Surface Morphology of Lithium Disilicate Glass-Ceramics and Highly Translucent Zirconia Ceramics. *Materials* **2022**, *15*, 3614. [\[CrossRef\]](#) [\[PubMed\]](#)
114. Borges, G.A.; Sophr, A.M.; De Goes, M.F.; Sobrinho, L.C.; Chan, D.C. Effect of etching and airborne particle abrasion on the microstructure of different dental ceramics. *J. Prosthet. Dent.* **2003**, *89*, 479–488. [\[CrossRef\]](#) [\[PubMed\]](#)
115. Ho, G.W.; Matinlinna, J.P. Evaluation of the microtensile bond strength between resin composite and hydrofluoric acid etched ceramic in different storage media. *J. Adhes. Sci. Technol.* **2011**, *25*, 2671–2685. [\[CrossRef\]](#)
116. França, R.; Bebsch, M.; Haimeur, A.; Fernandes, A.C.; Sacher, E. Physicochemical surface characterizations of four dental CAD/CAM lithium disilicate-based glass ceramics on HF etching: An XPS study. *Ceram. Int.* **2020**, *46*, 1411–1418. [\[CrossRef\]](#)
117. Kalavacharla, V.K.; Lawson, N.C.; Ramp, L.C.; Burgess, J.O. Influence of Etching Protocol and Silane Treatment with a Universal Adhesive on Lithium Disilicate Bond Strength. *Oper. Dent.* **2015**, *40*, 372–378. [\[CrossRef\]](#) [\[PubMed\]](#)
118. Zogheib, L.V.; Bona, A.D.; Kimpara, E.T.; McCabe, J.F. Effect of hydrofluoric acid etching duration on the roughness and flexural strength of a lithium disilicate-based glass ceramic. *Braz. Dent. J.* **2011**, *22*, 45–50. [\[CrossRef\]](#)
119. Hooshmand, T.; Parvizi, S.; Keshvad, A. Effect of surface acid etching on the biaxial flexural strength of two hot-pressed glass ceramics. *J. Prosthodont.* **2008**, *17*, 415–419. [\[CrossRef\]](#) [\[PubMed\]](#)
120. Xiaoping, L.; Dongfeng, R.; Silikas, N. Effect of etching time and resin bond on the flexural strength of IPS e. max Press glass ceramic. *Dent. Mater.* **2014**, *30*, e330–e336. [\[CrossRef\]](#) [\[PubMed\]](#)
121. Menees, T.S.; Lawson, N.C.; Beck, P.R.; Burgess, J.O. Influence of particle abrasion or hydrofluoric acid etching on lithium disilicate flexural strength. *J. Prosthet. Dent.* **2014**, *112*, 1164–1170. [\[CrossRef\]](#) [\[PubMed\]](#)
122. Guarda, G.B.; Correr, A.B.; Gonçalves, L.S.; Costa, A.R.; Borges, G.A.; Sinhoreti, M.A.; Correr-Sobrinho, L. Effects of surface treatments, thermocycling, and cyclic loading on the bond strength of a resin cement bonded to a lithium disilicate glass ceramic. *Oper. Dent.* **2013**, *38*, 208–217. [\[CrossRef\]](#) [\[PubMed\]](#)
123. Maruo, Y.; Nishigawa, G.; Irie, M.; Yoshihara, K.; Matsumoto, T.; Minagi, S. Does acid etching morphologically and chemically affect lithium disilicate glass ceramic surfaces? *J. Appl. Biomater. Funct. Mater.* **2017**, *15*, 93–100. [\[CrossRef\]](#) [\[PubMed\]](#)
124. Sundfeld, D.; Correr-Sobrinho, L.; Pini, N.I.P.; Costa, A.R.; Sundfeld, R.H.; Pfeifer, C.S.; Martins, L.R. The effect of hydrofluoric acid concentration and heat on the bonding to lithium disilicate glass ceramic. *Braz. Dent. J.* **2016**, *27*, 727–733. [\[CrossRef\]](#) [\[PubMed\]](#)

125. Cuzic, C.; Jivanescu, A.; Negru, R.M.; Hulka, I.; Rominu, M. The Influence of Hydrofluoric Acid Temperature and Application Technique on Ceramic Surface Texture and Shear Bond Strength of an Adhesive Cement. *Materials* **2023**, *16*, 4303. [[CrossRef](#)] [[PubMed](#)]
126. Leyva Del Rio, D.; Sandoval-Sanchez, E.; Campos-Villegas, N.E.; Azpiazu-Flores, F.X.; Zavala-Alonso, N.V. Influence of Heated Hydrofluoric Acid Surface Treatment on Surface Roughness and Bond Strength to Feldspathic Ceramics and Lithium-Disilicate Glass-Ceramics. *J. Adhes. Dent.* **2021**, *23*, 549–555. [[PubMed](#)]
127. Bagheri, H.; Hooshmand, T.; Aghajani, F. Effect of Ceramic Surface Treatments after Machine Grinding on the Biaxial Flexural Strength of Different CAD/CAM Dental Ceramics. *J. Dent.* **2015**, *12*, 621–629.
128. Loomans, B.A.; Mine, A.; Roeters, F.J.; Opdam, N.J.; De Munck, J.; Huysmans, M.C.; Van Meerbeek, B. Hydrofluoric acid on dentin should be avoided. *Dent. Mater.* **2010**, *26*, 643–649. [[CrossRef](#)] [[PubMed](#)]
129. Ayad, M.F.; Fahmy, N.Z.; Rosenstiel, S.F. Effect of surface treatment on roughness and bond strength of a heat-pressed ceramic. *J. Prosthet. Dent.* **2008**, *99*, 123–130. [[CrossRef](#)] [[PubMed](#)]
130. Bajraktarova-Valjakova, E.; Grozdanov, A.; Guguvcevski, L.; Korunoska-Stevkovska, V.; Kapusevska, B.; Gigovski, N.; Mijoska, A.; Bajraktarova-Misevska, C. Acid etching as surface treatment method for luting of glass-ceramic restorations, part 1: Acids, application protocol and etching effectiveness. *Open Access Maced. J. Med. Sci.* **2018**, *6*, 568. [[CrossRef](#)] [[PubMed](#)]
131. Lopes, G.C.; Perdigão, J.; Baptista, D.; Ballarin, A. Does a Self-etching Ceramic Primer Improve Bonding to Lithium Disilicate Ceramics? Bond Strengths and FESEM Analyses. *Oper. Dent.* **2019**, *44*, 210–218. [[CrossRef](#)] [[PubMed](#)]
132. Tribst, J.P.; Diamantino, P.J.; de Freitas, M.R.; Tanaka, I.V.; Silva-Concílio, L.R.; de Melo, R.M. Effect of active application of self-etching ceramic primer on the long-term bond strength of different dental CAD/CAM materials. *J. Clin. Exp. Dent.* **2021**, *13*, e1089–e1095. [[CrossRef](#)] [[PubMed](#)]
133. Tribst, J.; Anami, L.C.; Özcan, M.; Bottino, M.A.; Melo, R.M.; Saavedra, G. Self-etching Primers vs Acid Conditioning: Impact on Bond Strength Between Ceramics and Resin Cement. *Oper. Dent.* **2018**, *43*, 372–379. [[CrossRef](#)] [[PubMed](#)]
134. Souza, R.; da Silva, N.R.; de Miranda, L.M.; de Araújo, G.M.; Moura, D.; Barbosa, H. Two-year Follow-up of Ceramic Veneers and a Full Crown Treated With Self-etching Ceramic Primer: A Case Report. *Oper. Dent.* **2020**, *45*, 352–358. [[CrossRef](#)] [[PubMed](#)]
135. Schestatsky, R.; Zucuni, C.P.; Venturini, A.B.; de Lima Burgo, T.A.; Bacchi, A.; Valandro, L.F.; Pereira, G.K.R. CAD-CAM milled versus pressed lithium-disilicate monolithic crowns adhesively cemented after distinct surface treatments: Fatigue performance and ceramic surface characteristics. *J. Mech. Behav. Biomed. Mater.* **2019**, *94*, 144–154. [[CrossRef](#)] [[PubMed](#)]
136. Sriamporn, T.; Kraisintu, P.; See, L.P.; Swasdison, S.; Klaisiri, A.; Thamrongananskul, N. Effect of Different Neutralizing Agents on Feldspathic Porcelain Etched by Hydrofluoric Acid. *Eur. J. Dent.* **2019**, *13*, 75–81. [[CrossRef](#)] [[PubMed](#)]
137. Panah, F.G.; Rezai, S.M.; Ahmadian, L. The influence of ceramic surface treatments on the micro-shear bond strength of composite resin to IPS Empress 2. *J. Prosthodont.* **2008**, *17*, 409–414. [[CrossRef](#)] [[PubMed](#)]
138. Wang, X.; Zhang, Y.; Ni, L.; You, C.; Ye, C.; Jiang, R.; Liu, L.; Liu, J.; Han, C. A review of treatment strategies for hydrofluoric acid burns: Current status and future prospects. *Burns* **2014**, *40*, 1447–1457. [[CrossRef](#)] [[PubMed](#)]
139. Özcan, M.; Volpato, C. Surface conditioning protocol for the adhesion of resin-based materials to glassy matrix ceramics: How to condition and why. *J. Adhes. Dent.* **2015**, *17*, 292–293. [[PubMed](#)]
140. Saavedra, G.; Arik, E.K.; Federico, C.D.; Galhano, G.; Zamboni, S.; Baldissara, P.; Bottino, M.A.; Valandro, L.F. Effect of acid neutralization and mechanical cycling on the microtensile bond strength of glass-ceramic inlays. *Oper. Dent.* **2009**, *34*, 211–216. [[CrossRef](#)] [[PubMed](#)]
141. Bottino, M.; Snellaert, A.; Bergoli, C.; Özcan, M.; Bottino, M.; Valandro, L. Effect of ceramic etching protocols on resin bond strength to a feldspar ceramic. *Oper. Dent.* **2015**, *40*, E40–E46. [[CrossRef](#)] [[PubMed](#)]
142. Ramakrishnaiah, R.; Alkheraif, A.A.; Divakar, D.D.; Alghamdi, K.F.; Matinlinna, J.P.; Lung, C.Y.K.; Cherian, S.; Vallittu, P.K. The effect of lithium disilicate ceramic surface neutralization on wettability of silane coupling agents and adhesive resin cements. *Silicon* **2018**, *10*, 2391–2397. [[CrossRef](#)]
143. Asiry, M.A.; AlShahrani, I.; Alaqeel, S.M.; Durgesh, B.H.; Ramakrishnaiah, R. Effect of two-step and one-step surface conditioning of glass ceramic on adhesion strength of orthodontic bracket and effect of thermo-cycling on adhesion strength. *J. Mech. Behav. Biomed. Mater.* **2018**, *84*, 22–27. [[CrossRef](#)] [[PubMed](#)]
144. Sato, T.d.P.; Cotes, C.; Yamamoto, L.T.; Rossi, N.R.; da Cruz Macedo, V.; Kimpara, E.T. Flexural strength of a pressable lithium disilicate ceramic: Influence of surface treatments. *Appl. Adhes. Sci.* **2013**, *1*, 7. [[CrossRef](#)]
145. Benetti, A.R.; Papia, E.; Matinlinna, J.P. Bonding ceramic restorations. *Nor. Tann. Tid.* **2019**, *129*, 30–36. [[CrossRef](#)]
146. Cho, B.-H.; Han, G.-J.; Oh, K.-H.; Chung, S.-N.; Chun, B.-H. The effect of plasma polymer coating using atmospheric-pressure glow discharge on the shear bond strength of composite resin to ceramic. *J. Mater. Sci.* **2011**, *46*, 2755–2763. [[CrossRef](#)]
147. Ito, Y.; Okawa, T.; Fukumoto, T.; Tsurumi, A.; Tatsuta, M.; Fujii, T.; Tanaka, J.; Tanaka, M. Influence of atmospheric pressure low-temperature plasma treatment on the shear bond strength between zirconia and resin cement. *J. Prosthodont. Res.* **2016**, *60*, 289–293. [[CrossRef](#)] [[PubMed](#)]
148. Birk, L.; Renner-Sitar, K.; Benčina, M.; Junkar, I. Dental silicate ceramics surface modification by nonthermal plasma: A systematic review. *Dent. Mater.* **2024**, *40*, 531–545. [[CrossRef](#)]
149. Itthipongsatorn, N.; Srisawasdi, S. Dentin microshear bond strength of various resin luting agents to zirconia-reinforced lithium silicate ceramics. *J. Prosthet. Dent.* **2020**, *124*, 237.e1–237.e7. [[CrossRef](#)] [[PubMed](#)]

150. Wang, Y.; Hui, R.; Gao, L.; Ma, Y.; Wu, X.; Meng, Y.; Hao, Z. Effect of surface treatments on bond durability of zirconia-reinforced lithium silicate ceramics: An in vitro study. *J. Prosthet. Dent.* **2022**, *128*, 1350.e1–1350.e10. [[CrossRef](#)] [[PubMed](#)]
151. Dalla-Nora, F.; Guilardi, L.F.; Zucuni, C.P.; Valandro, L.F.; Rippe, M.P. Fatigue Behavior of Monolithic Zirconia-Reinforced Lithium Silicate Ceramic Restorations: Effects of Conditionings of the Intaglio Surface and the Resin Cements. *Oper. Dent.* **2021**, *46*, 316–326. [[CrossRef](#)] [[PubMed](#)]
152. Al-Thagafi, R.; Al-Zordk, W.; Saker, S. Influence of Surface Conditioning Protocols on Reparability of CAD/CAM Zirconia-reinforced Lithium Silicate Ceramic. *J. Adhes. Dent.* **2016**, *18*, 135–141.
153. Madina, M.M.; Ozcan, M.; Badawi, M.F. Effect of surface conditioning and taper angle on the retention of IPS e.max Press crowns. *J. Prosthodont.* **2010**, *19*, 200–204. [[CrossRef](#)] [[PubMed](#)]
154. Nagaoka, N.; Yoshihara, K.; Tamada, Y.; Yoshida, Y.; Meerbeek, B.V. Ultrastructure and bonding properties of tribochemical silica-coated zirconia. *Dent. Mater. J.* **2019**, *38*, 107–113. [[CrossRef](#)] [[PubMed](#)]
155. Jones, C.; Billington, R.; Pearson, G. The in vivo perception of roughness of restorations. *Br. Dent. J.* **2004**, *196*, 42–45. [[CrossRef](#)] [[PubMed](#)]
156. Bollen, C.M.; Papaioanno, W.; Van Eldere, J.; Schepers, E.; Quirynen, M.; Van Steenberghe, D. The influence of abutment surface roughness on plaque accumulation and peri-implant mucositis. *Clin. Oral Implant. Res.* **1996**, *7*, 201–211. [[CrossRef](#)] [[PubMed](#)]
157. Aksoy, G.; Polat, H.; Polat, M.; Coskun, G. Effect of various treatment and glazing (coating) techniques on the roughness and wettability of ceramic dental restorative surfaces. *Colloids Surf. B* **2006**, *53*, 254–259. [[CrossRef](#)]
158. Kurt, M.; Bankoğlu Güngör, M.; Karakoca Nemli, S.; Turhan Bal, B. Effects of glazing methods on the optical and surface properties of silicate ceramics. *J. Prosthodont. Res.* **2020**, *64*, 202–209. [[CrossRef](#)] [[PubMed](#)]
159. Kumchai, H.; Juntavee, P.; Sun, A.F.; Nathanson, D. Effect of glazing on flexural strength of full-contour zirconia. *Int. J. Dent.* **2018**, *2018*, 8793481. [[CrossRef](#)] [[PubMed](#)]
160. Anusavice, K.J. Standardizing failure, success, and survival decisions in clinical studies of ceramic and metal-ceramic fixed dental prostheses. *Dent. Mater.* **2012**, *28*, 102–111. [[CrossRef](#)] [[PubMed](#)]
161. Malamet, K.A.; Natto, Z.S.; Thompson, V.; Rekow, D.; Eckert, S.; Weber, H.-P. Ten-year survival of pressed, acid-etched e. max lithium disilicate monolithic and bilayered complete-coverage restorations: Performance and outcomes as a function of tooth position and age. *J. Prosthet. Dent.* **2019**, *121*, 782–790. [[CrossRef](#)] [[PubMed](#)]
162. Sailer, I.; Karasan, D.; Todorovic, A.; Ligoutsikou, M.; Pjetursson, B.E. Prosthetic failures in dental implant therapy. *Periodontol.* **2000** **2022**, *88*, 130–144. [[CrossRef](#)] [[PubMed](#)]
163. Kern, M.; Sasse, M.; Wolfart, S. Ten-year outcome of three-unit fixed dental prostheses made from monolithic lithium disilicate ceramic. *J. Am. Dent. Assoc.* **2012**, *143*, 234–240. [[CrossRef](#)] [[PubMed](#)]
164. Garling, A.; Sasse, M.; Becker, M.E.E.; Kern, M. Fifteen-year outcome of three-unit fixed dental prostheses made from monolithic lithium disilicate ceramic. *J. Dent.* **2019**, *89*, 103178. [[CrossRef](#)] [[PubMed](#)]
165. Wolfart, S.; Eschbach, S.; Scherrer, S.; Kern, M. Clinical outcome of three-unit lithium-disilicate glass-ceramic fixed dental prostheses: Up to 8 years results. *Dent. Mater.* **2009**, *25*, e63–e71. [[CrossRef](#)] [[PubMed](#)]
166. van den Breemer, C.R.; Vinkenborg, C.; van Pelt, H.; Edelhoff, D.; Cune, M.S. The Clinical Performance of Monolithic Lithium Disilicate Posterior Restorations after 5, 10, and 15 Years: A Retrospective Case Series. *Int. J. Prosthodont.* **2017**, *30*, 62–65. [[CrossRef](#)] [[PubMed](#)]
167. Fotiadou, C.; Manhart, J.; Diegritz, C.; Folwaczny, M.; Hickel, R.; Frasheri, I. Longevity of lithium disilicate indirect restorations in posterior teeth prepared by undergraduate students: A retrospective study up to 8.5 years. *J. Dent.* **2021**, *105*, 103569. [[CrossRef](#)]
168. Christensen, G. Zirconia: Most durable tooth-colored crown material in practice-based clinical study. *Clin. Rep.* **2018**, *11*, 1–3.
169. Zimmermann, M.; Koller, C.; Mehl, A.; Hickel, R. Indirect zirconia-reinforced lithium silicate ceramic CAD/CAM restorations: Preliminary clinical results after 12 months. *Quintessence Int.* **2017**, *48*, 19–25. [[PubMed](#)]
170. Rinke, S.; Pfitzenreuter, T.; Leha, A.; Roediger, M.; Ziebolz, D. Clinical evaluation of chairside-fabricated partial crowns composed of zirconia-reinforced lithium silicate ceramics: 3-year results of a prospective practice-based study. *J. Esthet. Restor. Dent.* **2020**, *32*, 226–235. [[CrossRef](#)] [[PubMed](#)]
171. Rinke, S.; Zuck, T.; Hausdörfer, T.; Leha, A.; Wassmann, T.; Ziebolz, D. Prospective clinical evaluation of chairside-fabricated zirconia-reinforced lithium silicate ceramic partial crowns—5-year results. *Clin. Oral Investig.* **2022**, *26*, 1593–1603. [[CrossRef](#)] [[PubMed](#)]
172. Ferrari, M.; Cagidiaco, E.F.; Goracci, C.; Sorrentino, R.; Zarone, F.; Grandini, S.; Joda, T. Posterior partial crowns out of lithium disilicate (LS2) with or without posts: A randomized controlled prospective clinical trial with a 3-year follow up. *J. Dent.* **2019**, *83*, 12–17. [[CrossRef](#)] [[PubMed](#)]
173. Degidi, M.; Nardi, D.; Sighinolfi, G.; Piattelli, A. Fixed Partial Restorations Made of a New Zirconia-Reinforced Lithium Silicate Material: A 2-Year Short-Term Report. *Int. J. Prosthodont.* **2021**, *34*, 37–46. [[CrossRef](#)] [[PubMed](#)]
174. Hölken, F.; Dietrich, H. Restoring Teeth with an Advanced Lithium Disilicate Ceramic: A Case Report and 1-Year Follow-Up. *Case Rep. Dent.* **2022**, *2022*, 6872542. [[CrossRef](#)] [[PubMed](#)]

175. Bompolaki, D.; Punj, A.; Fellows, C.; Truong, C.; Ferracane, J.L. Clinical Performance of CAD/CAM Monolithic Lithium Disilicate Implant-Supported Single Crowns Using Solid or Predrilled Blocks in a Fully Digital Workflow: A Retrospective Cohort Study With Up To 33 Months of Follow Up. *J. Prosthodont.* **2022**, *31*, 38–44. [[CrossRef](#)] [[PubMed](#)]
176. *BS EN ISO 6872:2015+A1:2018; Dentistry—Ceramic Materials*. International Organization for Standardization: Geneva, Switzerland, 2018.

Disclaimer/Publisher’s Note: The statements, opinions and data contained in all publications are solely those of the individual author(s) and contributor(s) and not of MDPI and/or the editor(s). MDPI and/or the editor(s) disclaim responsibility for any injury to people or property resulting from any ideas, methods, instructions or products referred to in the content.